



**HAL**  
open science

## One-step preparation procedure, mechanical properties and environmental performances of miscanthus-based concrete blocks

Colin Jury, Jordi Girones, Loan T.T. Vo, Erika Di Giuseppe, Grégory Mouille, Emilie Gineau, Stéphanie Arnoult, Maryse Brancourt-Hulmel, Catherine Lapierre, Laurent Cézard, et al.

### ► To cite this version:

Colin Jury, Jordi Girones, Loan T.T. Vo, Erika Di Giuseppe, Grégory Mouille, et al.. One-step preparation procedure, mechanical properties and environmental performances of miscanthus-based concrete blocks. *Materials Today Communications*, 2022, 31, pp.103575. 10.1016/j.mtcomm.2022.103575 . hal-03766074

**HAL Id: hal-03766074**

**<https://hal.inrae.fr/hal-03766074>**

Submitted on 22 Jul 2024

**HAL** is a multi-disciplinary open access archive for the deposit and dissemination of scientific research documents, whether they are published or not. The documents may come from teaching and research institutions in France or abroad, or from public or private research centers.

L'archive ouverte pluridisciplinaire **HAL**, est destinée au dépôt et à la diffusion de documents scientifiques de niveau recherche, publiés ou non, émanant des établissements d'enseignement et de recherche français ou étrangers, des laboratoires publics ou privés.



Distributed under a Creative Commons Attribution - NonCommercial 4.0 International License

1 **One-step preparation procedure, mechanical properties and environmental performances**  
2 **of miscanthus-based concrete blocks**

3

4 Colin Jury<sup>1\*</sup>, Jordi Girones<sup>2</sup>, Loan T. T. Vo<sup>2</sup>, Erika Di Giuseppe<sup>2</sup>, Grégory Mouille<sup>3</sup>, Emilie  
5 Gineau<sup>3</sup>, Stéphanie Arnoult<sup>4</sup>, Maryse Brancourt-Hulmel<sup>5</sup>, Catherine Lapierre<sup>3</sup>, Laurent Cézard<sup>3</sup>  
6 and Patrick Navard<sup>2\*</sup>

7

8 1- Inovertis-A3i, 255 rue Gustave Eiffel, 26290 Donzère, France

9 2- MINES ParisTech, PSL Research University, CEMEF\*\* - Centre de mise en forme des

10 matériaux, CNRS UMR 7635, CS 10207 rue Claude Daunesse 06904 Sophia Antipolis Cedex,

11 France

12 3- - Institut Jean-Pierre Bourgin, INRAE, AgroParisTech, Université Paris-Saclay, 78000,

13 Versailles, France

14 4 INRAE UE 0972 GCIE Picardie, Estrées-Mons 80203 Péronne, France

15 5 BioEcoAgro Joint Research Unit – INRAE AgroImpact - Université de Liège - Université de

16 Lille - Université de Picardie Jules Verne, Site d'Estrées-Mons CS 50136 80203 Péronne

17 cedex, France

18

19 \* Corresponding authors:

20 C. Jury Tel.: +33 (0)4 75 50 07 46

21 Email address: c.jury@inovertis.fr

22

23 P. Navard Tel.: +33 (0)4 93 95 74 66; Fax: +33 (0)4 92 38 97 52.

24 Email address: patrick.navard@mines-paristech.fr

25

26 \*\* Member of the European Polysaccharide Network of Excellence (EPNOE), [www.epnoe.eu](http://www.epnoe.eu)

27

28

29 **Highlights**

30

- 31 • Size of fragments important for blocks mechanical properties
- 32 • Low leaf/stem ratio is an important factor for improving mechanical properties
- 33 • Load-bearing miscanthus block worse for environment than conventional alternatives
- 34 • Climate change impact is not the only focus for developing biobased concretes
- 35 • Indirect consequences of Land Use Change important for environmental
- 36 performances

37

38

39 **Abstract**

40 Concrete blocks prepared with Portland cement and miscanthus-based aggregates were

41 prepared in order to check if the miscanthus genotype may influence their mechanical

42 properties and to perform an environmental assessment. To produce lightweight, load-

43 bearing concrete blocks using miscanthus stem fragments as aggregates in a single mixing

44 method turned out to be impossible, although trying to optimize the concrete formulation.

45 The results show that genotypes and size of miscanthus fragments controlled the mechanical

46 properties of the final blocks. The lower was the amount of light elements such as leaves and

47 sheath, the better were the mechanical properties of the blocks. When comparing

48 genotypes with the same leaf/stem ratio, it was not possible to see a correlation between

49 the biochemical composition of the stem and the compressive strength of the blocks. A  
50 probable explanation is the small variation of biochemical composition between genotypes.  
51 Using life cycle analysis tools, miscanthus block were not found to be competitive with  
52 conventional alternatives (concrete block and lightweight pumice block) when trying to  
53 increase compressive strength above 3 MPa. However, compared to non-load bearing  
54 alternatives (light clay brick), blocks integrating miscanthus had a better global  
55 environmental performance mainly due to a favorable climate change impact. The present  
56 work also points out the risk of decreasing the environmental performances when  
57 cultivating the crop on land in competition with food, because of the impacts of indirect  
58 consequences of Land Use Change.

59

60

## 61 **Keywords**

62 Miscanthus; Concrete; Life cycle assessment; Mechanical properties; Genotype

63

64

## 65 **1- Introduction**

66 The need for low environmental impact has led to a growing demand for novel concretes,  
67 with lightweight concretes (800-2000 kg/m<sup>3</sup>) being a possible option. They can be prepared  
68 in different manners [Li et al. 2019; Zeng et al. 2018; Dixit et al. 2019]. One of them consists  
69 in substituting part of the mineral aggregates with biomass materials, mostly extracted from  
70 plants. Compared to traditional materials, such plant-based construction materials can have  
71 several advantages such as the reduction of weight and of carbon emission, favorable  
72 hygrothermal and acoustical properties and better life cycle assessment and effects on

73 health [Chabanes et al. 2018; Saez-Perez et al. 2020; Liu et al. 2017; Barbieri et al. 2020].

74 Many scientific articles have been published, describing the use of a large variety of plant

75 materials such as hemp, coconut, jute, flax, sisal and many others, see for ex [Amziane &

76 Sonebi 2016; Saez-Perez et al. 2020; Onuaguluchi & Banthia 2016; Jami et al. 2019;

77 Alengaram et al. 2013]. Biomass fiber-reinforced concretes are interesting because they

78 have the potential of solving the expected progressive shortage of mineral resources

79 (including sands and gravels) [Yang et al. 2019]. However, the use of biomass-reinforced

80 concrete is limited due to the natural variations in the quality of biomass which may lead to

81 some unpredictability of the properties of the final products [Alengaram et al. 2013; Karade

82 et al. 2006; Merta & Tschegg 2013] and to chemical, physical and dimensional changes which

83 can occur within the natural fibers with time, hindering the dimensional stability and

84 mechanical properties of concretes [Tonoli et al. 2013; Bederina et al. 2012]. The main

85 reason for the lack of mechanical performance derives from biomass fibers being softer and

86 lacking the stiffness of the mineral aggregates they are replacing. As a result, the

87 compressive strength of biomass-reinforced concrete is poorer than that of conventional

88 concrete [Amziane & Sonebi 2016; Turgut 2007; Prusty et al. 2016; Çomak et al. 2018].

89 Among the many possibilities for choosing the plant from which organs or group of organs

90 will be used, miscanthus is a potentially good candidate. It is a perennial C4 grass requiring

91 low nitrogen inputs (Zapater et al. 2017), having a high aboveground biomass production

92 [Zub et al. 2011] and good mechanical properties of its stem fragments [Kaak and Schwarz,

93 2001; Kaack et al. 2003], which can be used for preparing polymer composites [Girones et al.

94 2016; Chupin et al. 2020]. The use of miscanthus was first explored by Pude et al (2002;

95 2003; 2004; 2005) for the preparation of plant-based concrete. They studied different

96 genotypes to select for concrete composite preparation those with low silicon content, in

97 combination with large cellulose and lignin contents to strengthen the stem fragments  
98 (called fibers afterwards). Other characteristics such as the amount of leave and the role of  
99 water from the initial fibers to the final concrete were considered. Their conclusions are that  
100 upon contact with water and cement, most of the water is absorbed by cellulose which is  
101 swelling in the sclerenchyma ring with water and cement rapidly migrating to the outer ring.  
102 Everything considered, including the fact that the permanent binding of water in the  
103 concrete is of great importance, they found that the best genotype maximizing all the  
104 needed parameters is *M. x giganteus*. Then, the preparation and properties of miscanthus-  
105 based concretes were further explored. Acikel (2011) added low amounts of miscanthus  
106 fibers in a sand, gravel, cement mixture and found that this was bringing an increase of the  
107 compressive strength of blocks of 4-10%. Merta and Tschegg (2013) compared the fracture  
108 energy of concrete reinforced with chopped fibres of hemp, wheat straw, and miscanthus.  
109 The latter increased the fracture energy of concrete by only 5%, far below the increase of  
110 70% observed with hemp, this being due to the low surface roughness, which limits stress  
111 transfer. Waldmann et al. (2016) prepared miscanthus-based concrete blocks where the  
112 miscanthus fibers were mineralized with various chemical substances like magnesite,  
113 calcium hydroxide, chalk and calcium chloride, the latter turning out to bring the best results  
114 in term of resistance to compression. Their mixtures had compressive strength in the same  
115 order as concretes prepared using other-than-vegetal aggregate lightweight concrete, from  
116 5 to 7 MPa when increasing the specific weight from 1000 to 1250 kg m<sup>-3</sup>. Courard and  
117 Parmentier (2017) looked at the carbonation effects of cement in the presence of  
118 miscanthus and to the effect of a pre-mineralization of the miscanthus fibers. They found  
119 that capturing CO<sub>2</sub> in concrete is an environmentally favorable process which allows to  
120 increase the abrasion resistance and the mechanical performances of concrete blocks. Chen

121 et al. (2017; 2020) measured the acoustic performances of miscanthus concrete. They found  
122 that ultra-light concretes (specific mass of about  $550 \text{ kg m}^{-3}$ ) with 30% v/v miscanthus fibers  
123 have a thermal conductivity of  $0.09 \text{ W m}^{-1} \text{ K}^{-1}$  and a high acoustic absorption coefficient (0.9)  
124 at low frequencies. The dosage and shape of miscanthus fibers have a significant effect on  
125 these properties. Ntimugara et al. (2020) looked at the possibilities for using miscanthus  
126 coming from Southwest England to develop building materials. Pereira Dias and Waldmann  
127 (2020) prepared miscanthus-based concrete varying water/cement ratio as well as the  
128 amount of miscanthus fibers, being pre-treated with a silica sealant or with a mixture of  
129 quartz and calcium hydroxide. The objective was to prepare loads-bearing blocks. A silica  
130 treatment, associated or not with an alkali extraction, was found to increase the  
131 compression strength [Boix et al 2016]. The main result of Pereira Dias and Waldmann  
132 (2020) study is that a silica sealant applied on the miscanthus fibers can be beneficial.  
133 Compressive strength in the order of 12-14 MPa was obtained for specific mass of over 1500  
134  $\text{kg m}^{-3}$ . As observed for all biomass-based concrete, increasing density of the mixture  
135 increases the compressive strength. Compressive strength of 5-8 MPa were obtained with  
136 specific masses around  $1000 \text{ kg m}^{-3}$ .

137 One of main issues for combining plant biomass with cement is the release of chemicals  
138 (mainly polysaccharides, sugar oligomers, sugars, lignin), extracted from the biofibers and  
139 reacting unfavorably with cement particles. When miscanthus fibers are placed in a cement-  
140 water-sand mixture, there is a large decrease of the cellulose and xylose content in the  
141 fibers, these two molecules being adsorbed on cement particles [Boix et al. 2020]. These  
142 results stress the importance of choosing the genotype and controlling the whole  
143 preparation process.

144 In all miscanthus-based concrete work, it is taken as granted that the use of miscanthus to  
145 prepare concrete is environmentally favorable but, despite many life cycle assessment (LCA)  
146 studies were performed on different uses (ethanol production, electricity, board, pellet,  
147 biochar, heat etc.) of miscanthus [Krzyżaniak et al. 2020, Lask at al. 2018, Fusi et al. 2020,  
148 Yesufu et al.2019, Tadele et al. 2019, Peric et al. 2018], no study having been performed on  
149 concrete reinforced miscanthus. However, looking to the various LCA studies on mainly  
150 hemp concrete, the environmental performances of bio-based concrete show a contrasted  
151 picture. A good performance on the climate change impact has always been demonstrated,  
152 although to a certain extend ( $-1.6 \text{ kg CO}_2\text{eq m}^{-2}$  to  $-36.08 \text{ CO}_2\text{eq m}^{-2}$ ) according to Arrigoni et  
153 al. (2017). However, the added value on the other impact categories is not always verified.  
154 Heidari et al. (2019) calculated around 20% better performances on human health and  
155 energy consumption but 300% worse performance on ecosystem quality compared to a  
156 reference wall. Prétot et al. (2014) highlights that hemp concrete may also generate a more  
157 significant impact on resources consumption, water consumption and water pollution in  
158 comparison to a brick wall and concrete blocks.

159 The purpose of this paper is to study the preparation, mechanical properties and life cycle  
160 assessment (LCA) performances of miscanthus-based concrete, prepared without pre-  
161 treatments of the biomass. Pre-treatments [Lo & Navard 2016] such as removal of  
162 extractives by alkali treatments or silanization can be too costly to be industrially  
163 implemented. Regarding LCA, the standardized methodology (ISO 14040/44) was used to  
164 evaluate the potential environmental impacts of a product, a process or a service. The  
165 objective was to compare the environmental performances of miscanthus reinforced blocks  
166 to conventional alternatives and identify how to improve them in a perspective of ecodesign.  
167 It is hypothesized that the genotype may influence the mechanical properties and that the



168 use of cement to reach load-bearing characteristics may be an obstacle to reach good  
169 environmental performances.

170

## 171 **2-Materials and methods**

172

### 173 **2.1 Raw materials**

174 Portland cements (52.5R CE CP2 NF by Calcia, Guerville, France) were stored in sealed  
175 containers to avoid moisture adsorption. Sands with two granular sizes of 0-2 and 0-4 mm  
176 were purchased from Castorama (Sophia Antipolis, France).

177 The vegetal aggregates used in this study are made of miscanthus stem fragments, broken,  
178 and cut at various lengths (1, 2 or 3 cm, with variable diameters of the fragments) by Fibres  
179 Recherche Développement FRD (Troyes, France). In order to study the influence of light parts  
180 of the stems (leave and sheath), leaves were removed on 1 cm fragments from H5 genotype.

181 Air was flown horizontally to a stream of miscanthus fibers falling from a controlled height.

182 Heavy fragments will not change their trajectory and continue their linear fall, whereas  
183 lighter fragments will be pushed away. Thus, the fragments can be separated by controlling  
184 the speed of the air blown, the distance from the floor at which the air is blown, and the  
185 distance between the collection point and the floor. Stems, either with or without leave,  
186 were used. Fragments are thus mixtures of tissues and their composition varies since the  
187 biochemical characteristics are depending on the location of internodes. To be in line with  
188 literature on this topic, these stem fragments will be called fibers in all this article.

189 Two types of experiments were conducted. A first set of experiments was dedicated to study  
190 the preparation of miscanthus-based concrete blocks and to the life cycle assessments. This  
191 was performed with a *Miscanthus × giganteus* genotype planted in Ecurie des Prés Hauts

192 (France) and harvested in September 2014. This sample will be called “Granulo Mg” in the  
193 following. The size distribution of Granulo Mg fragments is shown in Figure 1S.

194 A second set of experiments was used to explore the genotype effect. Six contrasted  
195 genotypes were chosen to offer wide phenotypic variability and their origin is given in Table  
196 1S. Two of the genotypes were *M. x giganteus* interspecific hybrids: a biomass genotype  
197 (coded GiGB) and the Floridulus (Flo) ornamental variety. Two other genotypes were  
198 varieties from the *M. sinensis* species: a biomass tetraploid Goliath variety (Gol) and a  
199 diploid ornamental Malepartus variety (Mal). The two remaining ones belonged to the *M.*  
200 *sacharriflorus* species: a biomass tetraploid (H5) and an ornamental diploid (Sac). The  
201 corresponding trial was a complete block design with three blocks and was planted by hand  
202 in spring 2007 at INRAE Estrées-Mons (Péronne, France) at a rhizome planting density of 2  
203 plants per m<sup>2</sup>. Each harvested plot consisted of 16 m<sup>2</sup> which contained four rows of eight  
204 plants and each plot was surrounded by a border row. The trial received no nitrogen input  
205 and weeds were regularly removed manually. No fertilizer and pesticides were applied. The  
206 harvest was carried out on a mature 8-year-old crop in February 2015 when the dry matter  
207 content reached 65% on average.

208 Granulo MG harvested in September 2014 was used for part 3.1 (Influence of preparation  
209 and process parameters) and 3.3 (Life cycle Assessment). The six genotypes harvested in  
210 Spring 2014 were used for Part 3.2 Effect of miscanthus genotypes and sizes).

211

## 212 **2.2 Concrete preparation, curing and testing**

213

### 214 **2.2.1 Preparation of the concrete mixtures and curing**

215 Water contents of sand and miscanthus fragments were measured by using a halogen  
216 moisture analyzer Mettler Toledo HX204 (Mettler Toledo, France) before each batch  
217 preparation. Drying temperature was set at 105 °C, and switch-off criterion to stop drying  
218 was less than 1 mg mass loss for a 50 second period. Approximately 30 kg of fresh concrete  
219 were prepared for each batch. Water was collected from the public drinking supply network.  
220 The amount of water added during mixing was adjusted depending on the amount of  
221 miscanthus fibers present in the mix. The water-to-cement ratio ranged between 0.59 and  
222 1.52. The total quantity of water in each mixture was measured as the amount of water  
223 added and the water contained as humidity in sand and miscanthus fibers. Concrete blocks  
224 were prepared in a laboratory conditioned at 20 °C. The proportion of cement / miscanthus /  
225 sand was varied.

226 The preparation of the concrete blocks was performed in one step, lasting about 20 min.  
227 Mixing was carried out in a Kniele KKM-L 30 mixer (Kniele, Germany). The order of  
228 component introduction was:

229 First, miscanthus and the pre-wetting water (40 wt% of miscanthus mass) were mixed.

230 Once the mix was homogenous, sand was added, followed by the incorporation of cement.

231 Finally, the rest of the needed water was added to the mixer gradually. Mixing time,

232 calculated from the moment the mixing water was added, lasted for 8 minutes. Then, the

233 fresh concrete mix was unloaded and concrete blocks were immediately prepared. The

234 needed amount of the fresh mix was poured into a 15×15×15 cm<sup>3</sup> metallic mold, attached

235 to a vibration table (Netter Vibration NV, Germany). Demolding oil (Deltapro, France) was

236 sprayed into the mold before fresh concrete was poured in. Concrete blocks were formed

237 under the vibration-compaction method. Samples were vibrated with a frequency of 50 Hz

238 while being simultaneously compacted with a hammer. Time for vibration-compaction

239 varied from 20 sec to 90 sec, depending on the characteristics of the concrete mix. After  
 240 demolding, the concrete blocks were stored in a temperature-controlled room at 20°C and  
 241 covered with a plastic sheet for 7 days.

242 Various mixtures were tested to investigate the effect of miscanthus/cement/sand contents  
 243 on the compression strength of the obtained concretes (Table 1). Based on dry mass,  
 244 miscanthus Granulo MG content in the concrete was varied from 5 wt% to 12 wt%, whereas  
 245 cement content was varied from 20 wt% to 40 wt%, the rest of the mixture being sand and  
 246 water.

247 Table 1: Composition of concrete mixes (final total mass 1000 kg).

248

Cement (kg)	Miscanthus (kg)	Sand (kg)	Water-to-binder ratio
400	120	480	0.71
	96	504	0.66
	72	528	0.59
300	120	580	0.94
	91	609	0.84
	62	638	0.70
200	120	680	1.52
	86	714	1.22
	52	748	1.04

249

### 250 2.2.2 Testing

251 At the end of the curing period, the specimens were weighted, and their dimensions were  
 252 measured with a Vernier caliper (precision 0.1 mm). Dimensions were used to calculate the  
 253 volume. The compressive tests were conducted on a hydraulic DARTEC HA 250 instrument  
 254 (Zwick, Germany) at constant deformation speed of 5 mm/s, measuring force and  
 255 displacement, used to calculate stress and deformation.

256 The volume change of a concrete block in percentage (%) was calculated according to the  
 257 equation:

258 
$$\text{Volume change (\%)} = \frac{V_7 - V_0}{V_0} \times 100\%$$

259 where  $V_7$  and  $V_0$  are the volume of the concrete block at 7 and 0 days, respectively.

260 To check the effect of block orientation upon the mechanical properties, a set of 5 cubes  
261 were prepared with Granulo MG miscanthus fibers in the same conditions and their  
262 mechanical properties were measured by applying load on two different orientations, being  
263 axial compression at  $0^\circ$  and perpendicular compression at  $90^\circ$  towards the compaction  
264 direction (Figure 2S).

265

### 266 2.2.3 Reference composition

267 A reference composition will be used for all comparisons between different preparation  
268 procedures. The reference composition was arbitrary set as 40 wt% cement, 48 wt% sand  
269 and 12 wt% miscanthus (based on dry mass) with a total water-to-binder ratio of 0.64.

270

### 271 2.3 Biomass composition

272 The dry miscanthus samples were ground and sieved at 0.1 mm before exhaustive water,  
273 then ethanol extraction in a Soxhlet apparatus. The recovered extractive-free samples,  
274 corresponding to cell wall (CW) samples, were dried at  $50^\circ\text{C}$  before their compositional  
275 analyses. The lignin content (ABL) was measured using the acetyl bromide lignin method  
276 according to Sibout et al. (2016). Lignin composition was determined from the relative  
277 percentage of the *p*-hydroxyphenyl (H), guaiacyl (G), and syringyl (S) monomers released by  
278 thioacidolysis of CW samples, as described in (Méchin et al. 2014).

279 The hemicellulose and cellulose levels as well as the hemicellulosic neutral sugars were  
280 measured as described in (Chupin et al., 2017) and from 10 mg of the aforementioned dried

281 CW samples. The CW samples were kept in 2.5 M trifluoroacetic acid (TFA) for 1.5 h at 100  
282 °C. To determine the cellulose content, the residual pellet obtained after the TFA hydrolysis  
283 was rinsed twice with ten volumes of water and hydrolyzed with H<sub>2</sub>SO<sub>4</sub>. The  
284 monosaccharides released by TFA and H<sub>2</sub>SO<sub>4</sub> hydrolysis were diluted a minimum of 500  
285 times and quantified using an HPAEC-PAD chromatograph. 20 mg DW of ground samples  
286 were then extracted in 1 mL 80% ethanol for 30 min at 78 °C, then centrifuged (1000 rpm).  
287 The supernatant containing sugars was placed in 50 mL graduated flask. The pellet was  
288 suspended in 1 mL of 80% ethanol in same condition as previously, this procedure being  
289 carried out 3 times. After homogenization and aliquot filtration through membrane filter  
290 0.22 µm, the mono and di saccharide contents were quantified using an HPAEC-PAD  
291 chromatograph. The separation was carried out by Car-boPack PA1 Column at 30 °C with an  
292 isocratic elution of 150 mM sodium hydroxide. The hemicellulosic neutral sugars  
293 characterized were the following: arabinose (Ara), galactose (Gal), glucose (Glc), rhamnose  
294 (Rha), and xylose (Xyl). The glucose (Glc) from cellulose was also measured. The main  
295 phenolic acids, ester-linked *p*-coumaric acid (CA) and ferulic acid (FA) were measured by mild  
296 alkaline hydrolysis, followed by solid phase extraction and then HPLC analyses according to  
297 (Ho-Yue-Kuang et al., 2016). For HPLC separation, 1 µl of sample was injected onto an RP18  
298 column (4×50mm, 2.7 µm particle size, Nucleoshell, Macherey-Nagel) with a flow rate of 0.5  
299 ml/min. The eluents were 0.1% formic acid in water (A) and 0.1% formic acid in acetonitrile  
300 (B), and the gradient was as follows: 0–3 min, 0% B; 12 min, 20% B; 14 min, 80% B; 16 min,  
301 0% B. The quantitative determination of alkali-released CA and FA was performed from the  
302 250–400 nm DAD chromatograms and after calibration with authentic compounds.

303 The composition and leaf/stem ratio of the six genotypes are given in Table 2S. To approach  
304 at best the mean composition of the whole stem while composition measurements are

305 performed on small amounts of samples, the composition used in the following of the paper  
306 was the mean value of the composition of the top and the bottom internodes of each  
307 genotype.

308

## 309 **2.4 Statistics**

310 The experimental design allowed to compare six genotypes for strength measured at 7 and  
311 28 days as well as volume change. The corresponding ANOVA included the genotype effect  
312 and the technical repetition effect. The three sizes of fragments, measured on the GIGB  
313 clone of *Miscanthus x giganteus*, were also compared for the same variables. Accordingly,  
314 the ANOVA included the size effect and the technical repetition effect. The comparison of  
315 genotype means as well as size means was based on the Student–Newman–Keuls test. All  
316 ANOVAs were based on the aov function of agricolae package and the SNK comparisons on  
317 the SNK.test function. For all statistical tests, the probability level was considered at 0.05.

318

## 319 **2.5 Life Cycle Assessment**

320

### 321 **2.5.1 Notation used in the life cycle assessment studies**

322 Acidif. (Acidification); Clim. Chang. Excl. (Climate change excluding biogenic carbon); Ecotox.  
323 Freshwat. (Ecotoxicity freshwater); Eutr. Freshwat. (Eutrophication freshwater); Eutr. Marine  
324 (Eutrophication marine); Eutr. Terres. (Eutrophication terrestrial); Hum. tox. Cancer (Human  
325 toxicity cancer); Hum. tox. non-cancer (Human toxicity non-cancer); Ion. rad. (Ionizing  
326 radiation); Land Use (Land use); Oz. Depl. Ozone depletion); Part. Mat. Form. (Particulate  
327 matter formation); Photoch. ozone form. (Photochemical ozone formation); Water dep.  
328 (Water depletion); Min., foss. & renew. Depl. (Mineral, fossil and renewable depletion).

329 The notations for the potential environmental impacts used in this study are reported in  
 330 Figures 6, 7, 8 and 10.

331

### 332 2.5.2 Functional unit and reference flows

333 The assessment was conducted for two different functions with the Granulo MG samples: (1)  
 334 non-load-bearing block with 4 MPa compression resistance and (2) load-bearing blocks with  
 335 6 MPa compression resistance, both with a specific mass at about 1000 kg m<sup>-3</sup>. These two  
 336 compression resistance values are based on norm NF EN 206-1. The minimum compression  
 337 resistance limit for load-bearing light blocks is 9 MPa for cubic test samples. It was  
 338 impossible to reach such value keeping the specific mass below 1000 kg m<sup>-3</sup>. So, the highest  
 339 attained resistance, 6MPa, was kept as the load-bearing limit to carry on the LCA analysis. It  
 340 must be noticed that cofunctions such as heat and acoustic insulation were not considered.  
 341 This is a limitation to the comparison between miscanthus and alternatives blocks. The  
 342 functional unit is 1 m<sup>2</sup> of wall keeping its function over 100 years. The reference flows for  
 343 each scenario are reported in Table 2.

344

345 Table 2: Function, functional units and reference flow for each scenario.

Function	Scenario	Functional unit and reference flow*
Non load-bearing scenario blocks	Miscanthus 8% DM	1 m <sup>2</sup> : 52 kg (44 blocks 40 mm thickness)
	clay bricks	1 m <sup>2</sup> : 34 kg (10 blocks 40 mm thickness)
Load-bearing scenario blocks	Miscanthus 5% DM	1 m <sup>2</sup> : 221 kg (44 blocks 150 mm thickness)
	100% concrete	1 m <sup>2</sup> : 178 kg (8 blocks 200 mm thickness)

346 \* Miscanthus blocks have 150/150 mm length and width, clay bricks 500/200 mm length and  
 347 width, full concrete blocks 500/250 mm length and width. DM stands for dry matter.



348

349 It is not expected that the production of miscanthus reinforced concrete blocks will have  
350 large-scale consequences on any markets. Thus, the LCA was performed according to  
351 methodology recommended by the European Union in the frame of the International Life  
352 Cycle Database (ILCD) [European Commission 2010] for a “Micro-level decision support”  
353 LCA’s type. This implies that background processes can be determined in an attributional  
354 way as well as that the co-function that cannot be solved by a subdivision of the system shall  
355 be solved in priority by the system expansion approach.

356

### 357 2.5.3 System boundaries and sub-scenarios

358 This is a cradle-to-grave LCA. It considers the main processes, resources consumption and  
359 waste from the production of blocks to the disposal of the wall in France as reported in  
360 Figure 1. The air drying is not considered because it does not require energy and resources.  
361 However, the infrastructure required for the drying is considered for the blocks production.  
362 The transportation phases are identified with the “T” letter. During the wall life, no  
363 maintenance is required. This step is nevertheless reported because of the carbonation  
364 process. The carbon uptake from atmosphere by the carbonation of the calcium oxide in  
365 concrete is calculated from [Pommer & Pade 2005]. To allow taking into account the delayed  
366 carbon storage over the 100 year’s timeframe of climate change impact evaluation method  
367 and life of the wall, the benefit of the carbon uptake from atmosphere is reduced by 50.5%  
368 according to the methodology recommended by the European Commission [European  
369 Commission 2010]. The carbon storage in miscanthus is also evaluated. 45% carbon in  
370 miscanthus dry mass was considered. The co-functions were solved according to the system  
371 expansion approach. The co-functions arise at the end-of-life when a fraction of the wall is

372 sorted and recycled as ballast. The assessment was performed in priority according to French  
373 conditions (e.g., electricity mix, agricultural machinery, etc.) then European (e.g., Portland  
374 cement production) or Switzerland (e.g., mortar production) and global (e.g., unspecified  
375 transport lorry) if no French datasets were available.

376

377 Figure 1: LCA system boundaries.

378

379 Sub scenarios have been considered for the miscanthus production. Two different yields of  
380 dry matter (DM) and agricultural practices have been modeled. A highly productive land  
381 with a  $14.8 \text{ t ha}^{-1} \text{ year}^{-1}$  DM (HighProdLand or HPL) and a lower productive land with  $6.4 \text{ t ha}^{-1}$   
382  $\text{year}^{-1}$  DM (LowProdLand or LPL) that requires fertilization. In the baseline scenario, neither  
383 direct nor indirect consequences of Land Use Change (dLUC/iLUC) are considered, miscanthus  
384 being cultivated more than 20 years on the same field not in competition with food  
385 production. It is assumed this scenario is the best representation of the performance of the  
386 miscanthus on a mid-term perspective, once the sector will develop at an industrial scale  
387 and where the dLUC and iLUC are no more relevant. Two additional scenarios were  
388 modeled. They represent the performances for the first 20 years of the miscanthus  
389 cultivation, before an equilibrium of the direct and indirect variation of the Soil Organic  
390 Carbon (SOC) stock is reached. The first scenario, called dLUC, considers that miscanthus is  
391 not in competition with food production and that it takes place on a land with a high SOC. In  
392 this case the cultivation leads to a SOC variation between  $-0.5$  to  $0 \text{ tC ha}^{-1} \text{ year}^{-1}$  over 20  
393 years [Ferchaud unpublished] thus to  $\text{CO}_2$  emissions. An average value of  $-0.25 \text{ tC ha}^{-1} \text{ year}^{-1}$   
394 was used. The second scenario, called d+iLUC, is representative of a miscanthus cultivation  
395 on a land in competition with food production. In this case the miscanthus is cultivated on a

396 land with a low SOC stock and it leads to a direct SOC variation between +0.2 to +0.6 tC ha<sup>-1</sup>  
397 year<sup>-1</sup> over 20 years [Ferchaud unpublished], implying a CO<sub>2</sub> storage. An average value of 0.4  
398 tC ha<sup>-1</sup> year<sup>-1</sup> was used. However, the indirect CO<sub>2</sub> emission due to indirect consequences of  
399 land use change are also taken into account. According to [Audsley et al., 2009; Schmidt et  
400 al., 2011; Flysjö et al. 2012] the indirect CO<sub>2</sub> emissions range from 1.43 to 8.58 t CO<sub>2</sub> ha<sup>-1</sup>  
401 year<sup>-1</sup>. An average value of 5.00 t CO<sub>2</sub> ha<sup>-1</sup> year<sup>-1</sup> was used (1.36 t ha<sup>-1</sup> year<sup>-1</sup> C). Moreover, as  
402 a rough estimation and to maximize impacts, it has also been assumed that the use of 1 ha  
403 to produce miscanthus in France instead of a food crop will be equivalent to the  
404 transformation and the occupation of 1 ha of tropical forest.

405

#### 406 2.5.4 Life cycle inventory, limitations and result calculations

407 The assessment was performed on the LCA software GaBi<sup>®</sup>. Table 3S reports the origin of the  
408 foreground and background data to calculate the life cycle inventories (LCI). The transport  
409 related to the supply of raw materials at each step as well as to the end-of-life is considered  
410 thanks to the average transport as defined in the Ecoinvent 3.3 database. The potential  
411 environmental impacts were calculated with the version 1.09 of the environmental impact  
412 evaluation set recommended by the European union in the frame of the ILCD [European  
413 Commission 2012].

414 The composition of the different block is reported in Table 4S (they have been slightly  
415 adapted from Table 1 for lightweight non load-bearing block and load-bearing block so to  
416 reach 4 MPa and 6 MPa).

417 The single score has been calculated using the ReCiPe method considering a Hierarchist and  
418 Average normalization and weighting set in European conditions [Goedkoop et al. 2012].

419 The three main expected limitations of this study were(1) that heat and acoustic insulation  
420 performances were not considered. The different alternatives were thus not compared on  
421 an equal basis; (2) the methodology to estimate nitrogen ( $\text{NO}_3^-$ ,  $\text{N}_2\text{O}$ ,  $\text{NH}_3$ ). Despite this was  
422 based on the one used in the Agribalyse database for the LCA of French crop production, it  
423 has to be kept in mind that this was not developed for permanent crop such as miscanthus;  
424 (3) the estimation of the consequences of iLUC could be improved a lot since some rough  
425 assumptions were made, i.e., that 1 ha of miscanthus cultivated in competition with food  
426 production replaces 1 ha of primary forest. But this last point should not play in favour of  
427 miscanthus since it can be expected that less than 1 ha would be replaced.

428

### 429 **3 Results and discussion**

430

#### 431 **3.1 Influence of preparation and process parameters (Granulo MG)**

432

##### 433 **3.1.1 Effect of orientation of the blocks during compression tests**

434 During the mold filling and subsequent compaction, the miscanthus fragments can be  
435 oriented. In addition, pressure is not homogeneously distributed. As a result, the mechanical  
436 properties of the concrete blocks may depend upon the orientation of the blocks during the  
437 compression tests. The maximum load sustained by the concrete blocks submitted to axial  
438 compression at  $0^\circ$  was  $2.4 \pm 0.2$  MPa while for the blocks compressed in the perpendicular  
439 direction  $90^\circ$ , this value is  $3.8 \pm 0.2$  MPa. These results evidenced that the mechanical  
440 properties of the test cubes are anisotropic. During mold filling, the miscanthus fibers are  
441 flowing in between the movement of sand and cement particles and it can be expected that  
442 their mean orientation to be either isotropic or slightly in the filling direction (which is

443 identical to the subsequent the compaction direction). Seen by eye, no specific direction can  
444 be spotted at this stage from the blocks' surfaces. But during the compaction, the overall  
445 movements of the mix are orienting miscanthus fibers perpendicular to the compaction  
446 direction, as can be seen by eye at the surface of the blocks. Fiber orientation in concrete  
447 has been widely studied in the case of steel fibers [see for ex Boulekbache et al. 2010;  
448 Lameiras et al. 2015; Ozyurt et al. 2007]. The flowability of concrete and its deformation  
449 history are influencing the distribution and orientation of the fibers which in turn trigger the  
450 mechanical property anisotropy through the intrinsic resistance of the individual fibers and  
451 the way crack energy is dissipated. A study of the fiber distribution and orientation inside the  
452 blocks was not performed but all blocks were simply marked after demolding in order to  
453 always test them in the perpendicular direction at 90°.

454

### 455 3.1.2 Effect of degree of compaction and sand sizes

456 A set of blocks with weights ranging from 4.2 to 4.9 kg per block, which represents a fresh  
457 concrete density of 1220 kg m<sup>-3</sup> to 1425 kg m<sup>-3</sup>, was prepared to estimate the optimal degree  
458 of compaction. Sand with a granulometry of 0-2 and 0-4 was used to investigate the effect of  
459 sand size on the mechanical properties. Increasing the amount of matter to increase blocks'  
460 weight increased the difficulty of block compaction. In addition, upon their removal from the  
461 mold, the blocks changed their dimensions, especially expanding their height. After 7 days of  
462 curing, the obtained blocks were tested for their compressive resistance. The results shown  
463 on Figure 2a evidenced the influence of the initial weight of the concrete blocks onto their  
464 dimensional stability and compression strength. The size of the blocks after seven days  
465 remained nearly stable for the blocks prepared with up to 4.8 kg. But blocks prepared above  
466 4.9 kg showed large dimensional changes. As a result, although the total load sustained was

467 the same as for the block of 4.8 kg, it gave a lower pressure resistance. These results pointed  
468 out that for the mode of preparation used, the optimal amount of fresh concrete was 4.8 kg  
469 per 15×15×15 cm<sup>3</sup> blocks.

470 The impact of sand size was also investigated. Figure 2b shows that the compression  
471 strength of the blocks was consistently lower when finer sand (0-2) were used for  
472 preparation of the concrete. Moreover, the blocks prepared with the finer sand suffered a  
473 higher deformation during the curing period than those prepared with the coarser sand. As a  
474 result, sand with the granular size of 0-4 was used for all subsequent preparation of concrete  
475 blocks.

476  
477 Figure 2: (a) Relationship between compressive strength/height of concrete block (sand 0-4)  
478 after 7 days and its weight (the initial height was 15 cm) and (b) mechanical properties of  
479 concrete blocks prepared with sand granulometry of 0-2 and 0-4.

480

### 481 3.1.3 Effect of miscanthus/cement/sand contents

482 Various mixtures were tested to investigate the effect of miscanthus/cement/sand contents  
483 on the compression strength of the obtained concretes (Table 1). The amount of water in  
484 the mix is a very important parameter for the overall properties of the concrete matrix.  
485 Excess water may induce phase separation and layer formation, while lack of water can  
486 reduce the workability and thus limit the compaction. Moreover, unlike mineral  
487 reinforcement materials, biomass can both absorb and release different amounts of water  
488 depending on their particle size and chemical compositions. In this work, the water-to-  
489 cement ratio was adjusted from 0.59 to 1.52 in order to obtain similar consistencies. It can  
490 be seen on Figure 3S that although there was only 5 to 12 wt% of miscanthus fibers in the

491 mixture, it accounts for from 30 % to 55 % of the total volume. Thus, the blocks prepared  
492 with concrete containing higher amount of miscanthus fibers had to be prepared at a lower  
493 density to achieve similar compaction, leading to blocks of  $1100 \text{ kg m}^{-3}$  to  $1475 \text{ kg m}^{-3}$   
494 specific masses (Figure 3). The mechanical properties of concrete showed a very clear  
495 dependency on miscanthus content. This can be explained by the fact that miscanthus  
496 biomass does not have good intrinsic mechanical properties, by the bulk density of  
497 miscanthus fragments and its effect onto the volume fraction in the concrete mix. Figure 3  
498 shows the decrease of compression strength with decreasing specific mass of the final  
499 concrete, a property observed with other biomass fillers [Waldmann et al., 2016]. Concrete  
500 with 12 wt% miscanthus had a compressive strength after 28 days in the order of 2-2.5 MPa.  
501 When it was reduced to 9 wt%, compressive resistance improved to 3.5-4.5 MPa and the  
502 best results (up to 8 MPa) were obtained for concrete mixes with 5-6 wt% miscanthus fibers.  
503  
504 Figure 3: Compressive strengths vs. specific mass of the concrete blocks after (a) 7 days and  
505 (b) 28 days.

506

### 507 **3.2 Effect of miscanthus genotypes and sizes (six genotypes)**

508 For testing the influence of miscanthus genotypes and sizes, the reference concrete mix (see  
509 section 2.2.2) was used. The water-to-binder ratio varied with the genotypes and sizes of the  
510 miscanthus fragments used in the mix, ranging from 0.65 to 0.81. Miscanthus stems cut to 1  
511 cm were used to evaluate the possible effect of genotypes. To suppress the influence of  
512 concrete density on the compression strength, the blocks were prepared at the same dry  
513 density ( $1\ 050 \text{ kg m}^{-3}$ , except for blocks reinforced with 3 cm GiGB fragments which was  $950$

514 kg m<sup>-3</sup>, due to the impossibility to compact more without having an immediate deformation  
515 of the block).

516

### 517 3.2.1 Influence of sizes and shapes of miscanthus fibers

518 The effect of fiber sizes was tested only for the GiGB genotype, which was cut to 1, 2 and 3  
519 cm (see Figure 4S).

520

521

522 Figure 4 and Table 3 shows the effect of the length of the fibers on the concrete  
523 compression for GiGB. When the length is increasing, the compression strength is strongly  
524 decreasing. Figure 4 is also showing the volume change of blocks at 7 days. Increasing the  
525 lengths of the fibers was associated with an increase of the volume of the blocks from  
526 preparation time till 7 days. This swelling of the blocks is probably due to forces exerted on  
527 groups of fibers which are accumulating frozen stresses released with time. The larger the  
528 fibers are, the more interactions they have with more possibilities of being out of  
529 equilibrium. Using small fibers could thus prevent this effect which is very much affecting the  
530 mechanical properties of blocks. Another effect is the ratio of the length of the reinforcing  
531 element to the size of the block. The larger this ratio is, the more difficult it is to properly fill  
532 the block, which could lead to stress build-up. From the above observation, it can be  
533 hypothesized that the differences in both the mechanical performance and dimension  
534 stability might lie in the capacity of the smaller fragments to be compacted and fill voids.

535



536 Figure 4: (a) Strain-stress curves at 28 days of the concretes reinforced with fibers from  
537 different sizes and (b) their compressive strengths at 7 and 28 days (bars) and volume  
538 change at 7 days (●).

539

540 Table 3: ANOVA table comparing 3 sizes of fragments for *M. giganteus* (coded GIGB in Table  
 541 1S) measured at 7 and 28 days (in GPa) and volume change (in %). Means genotype  
 542 comparisons are based on Student–Newman–Keuls test (SNK) and means followed by a  
 543 same letter are not significantly different at 0.05 probability level.

544

Variable	Strength at 7 days (GPa)			Strength at 28 days (GPa)			Volume change (%)			
	Effect	Df	F value	Pr(>F)	F value	Pr(>F)	F value	Pr(>F)		
Size	2	56.11	0.001185	*	39.99	0.002269	*	67.94	0.000818	*
Repetition	2	18.87	0.009182	ns	1.26	0.375380	ns	2.34	0.212339	ns
Residuals	4									

Size	Means	SNK groups	Means	SNK groups	Means	SNK groups
1	1.51	a	1.91	a	8.22	c
2	1.38	b	1.51	b	12.56	b
3	1.12	c	1.16	c	14.40	a
Mean	1.34		1.53		11.73	
CV (%)	3.40		6.70		5.69	

\* significant at 0.05 probability level  
 ns = non significant

545

### 546 3.2.2 Influence of genotype on compression strength

547 Figure 5 and Table 5 show the effect of miscanthus genotype on the compression strength of  
 548 the blocks keeping length of fibers and density of block constant. On Figure 5a, a difference  
 549 in the compressive load – deformation curves at 28 days can be seen. For the blocks having  
 550 the best compression strength (H5, GiGB and Flo), there is a bend at the knee region of the  
 551 load-deformation curves. For the three other genotypes (Mal, Sac and Gol), the shape of the  
 552 curve is different, with a plateau up to the breaking point. A similar effect was observed

553 when considering the different fiber lengths, as shown on Figure 4. Miscanthus-reinforced  
554 concretes can be considered as a ductile material with miscanthus fibers acting as the  
555 reinforcement. The shape with a clear bend at the knee region suggests a better bond  
556 between miscanthus fibers and cement matrix, allowing an enhanced load transfer from the  
557 cement towards the miscanthus fibers. As a result, the concrete blocks could withstand an  
558 additional load at lower deformation levels.

559

560 Figure 5: (a) Compressive load – deformation curves at 28 days of the concretes reinforced  
561 with fragments from different genotypes and (b) their compressive strengths at 7 and 28  
562 days (bars) and volume change at 7 days (●).

563

564

565 Table 4: ANOVA table comparing 6 genotypes for strength measured at 7 and 28 days (in  
566 GPa) and volume change (in %). Means genotype comparisons are based on the Student–  
567 Newman–Keuls test (SNK) and means followed by a same letter are not significantly  
568 different at 0.05 probability level.

569

Variable		Strength at 7 days			Strength at 28 days			Volume change		
Effect	Df	F value	Pr(>F)		F value	Pr(>F)		F value	Pr(>F)	
Genotypes	5	100.61	0,0000005	*	114.51	0.0000003	*	87.05	0.0000009	*
Repetition	2	1.28	0,328315	ns	0.42	0.673135	ns	1.19	0.352703	ns
Residuals	8									

Genotypes	Means	SNK groups	Means	SNK groups	Means	SNK groups
H5	1.67	a	2.03	a	3.77	e
GiGB	1.51	a	1.91	a	8.22	c
FLO	1.50	a	1.62	b	6.47	d
Mal	0.91	b	1.35	c	12.13	b
Sac	0.46	c	0.80	d	13.70	a
Gol	0.32	c	0.45	e	12.15	b
Mean	1.11		1,0		8.97	
CV (%)		8.72		7.04		7.49

\* significant at 0.05 probability level

ns = non significant

572

573 Results of Figure 5 and Table 4 show a clear correlation between the dimensional stability of  
574 the obtained concretes and their compressive strength. Concretes with low mechanical  
575 performance suffered a higher volume increase during setting, ranging from 12 to 14%. By  
576 the opposite, the volume increases for the concretes reinforced with H5, Flo, and GiGB was  
577 limited from 3 to 8 %. An explanation for this correlation could be the formation of cracks  
578 and internal structural damages in the concrete caused during the expansion of the material  
579 before the cement was cured.

580 During the preparation of the stem fragment from individual *miscanthus* plants, leaf blades,  
581 leaf sheaths and stems are separated and mixed up. The leaf blades and sheaths being  
582 lighter, they represent a larger volume fraction. As a result, analysis of the fibers evidenced  
583 that the *miscanthus* samples containing higher proportions of leave and sheaths presented a  
584 lower bulk density than those consisting mostly of stem fragments. Since all concretes were  
585 prepared at the similar density, those prepared with the lower bulk density fragments had to  
586 be compressed more to reach the required sample dimensions. As a result of this higher  
587 compression degree, they might have a larger tendency to increase their size (dimensional  
588 changes) to release the stresses accumulated during compression leading to the internal  
589 cracks, hence leading to lower mechanical performance. Indeed, as it can be noticed in  
590 Figure 5 the evolution of compressive strength at 7 days presents a clear correlation with the  
591 bulk density of *miscanthus* fibers used as the reinforcement, with compressive strength  
592 increasing with bulk density. Since no fiber selection was conducted, the bulk density of  
593 *miscanthus* samples was strongly influenced by the leaf/stem ratio of their individual plants.  
594 Thus, the stronger concretes were prepared with the genotypes with higher bulk density  
595 (H5, GiGB and Flo) and a lower leaf/stem ratio (Table 2S).

596

### 597 3.2.3 Correlations between density, biochemical composition and compression strength

598 A comparison between the biochemical composition and the compression strength is  
599 difficult since the different genotypes have different densities, linked to the presence of  
600 different quantities of leaves. This has a very strong influence on the mechanical properties,  
601 as shown on Table 5. The denser genotypes, (H5, GiGB, Flo) have the best mechanical  
602 properties compared with the lighter ones (Mal and Sac). The situation for Gol is different,  
603 for unknown reasons.

604

605 Table 5: Compressive strength (MPa)of concrete prepared with the six genotypes.

Genotype	H5	GiGB	Flo	Mal	Sac	Gol
Leaf/stem ratio	0.04	0.04	0.05	0.22	0.31	0.08
Strength	1.67	1.51	1.50	0.90	0.46	0.32

606

607 To compare the biochemical composition of the six genotypes with the mechanical  
608 properties of the concrete blocks has no sense if the leaf/stem ratio is not considered. Thus,  
609 only the three genotypes having a low amount of leaves was considered in order to keep a  
610 group of miscanthus clones with similar structural characteristics. Table 6 gives the  
611 correlation results showing that none of the correlation coefficients are significant at the  
612 probability level of 0.05. This means that none of the composition parameters has an  
613 influence on the compressive strength of the prepared concrete. A plausible reason is that  
614 the variation of chemical composition is too low to be effective on cement setting. This

615 result is similar to the only published results on the influence of miscanthus genotypes on  
616 concrete properties (Pude et al 2005).

617

618

619 Table 6: Correlation matrix between cell wall (CW) composition and compressive strength  
 620 for H5, GiGB and Flo. N = 18; ns: non significant at p= 0.05. ABL: Acetyl Bromide Lignin; CA: *p*-  
 621 coumaric acid; FA: ferulic acid. H, G and S : *p*-hydroxyphenyl (H), guaiacyl (G) and syringyl (S)  
 622 thioacidolysis monomers. Rha, Gal, Glc, Ara and Xyl: Rhamnose, galactose, glucose, arabinose  
 623 and xylose.  
 624

Compositional parameter	Strength 7 days	Strength 28 days
Lignin content (% ABL by wt)	0.1 ns	0.34 ns
Phenolic acids ester-linked to the CW		
CA	0.43 ns	0.39 ns
FA	0.1 ns	0.34 ns
Relative % of lignin-derived H, G and S thioacidolysis monomers		
H	0 ns	-0.07 ns
G	0 ns	0 ns
S	0 ns	0 ns
Neutral sugars from hemicellulosic polysaccharides		
Rha	-0.22 ns	-0.13 ns
Gal	-0.2 ns	-0.4 ns
Glc	-0.1 ns	-0.2 ns
Ara	0 ns	0 ns
Xyl	0 ns	0 ns
Total	0 ns	0 ns
Glc from cellulose	0.22 ns	0.13 ns

625

626 3.2.4 Effect of light fraction removal



627 The previous results show that bulk density of miscanthus fibers play a crucial role on the  
628 overall compressive strength of the obtained concretes. To corroborate this aspect, a series  
629 of tests were conducted in which the lighter fractions of the fibers (leave and sheath pieces)  
630 was removed. 1cm fragments from H5 genotype were chosen for this investigation. The  
631 reference concrete mix (section 2.2.3) was used, and the water-to-cement ratio was 0.76.  
632 The concrete blocks were prepared at the same dry density of 1.05. The influence of sieving  
633 (pore size: 5 mm) was also tested, with the separation based on size. It was assumed that  
634 considering their strength, the fragments from the stem would remain relatively larger  
635 during grinding and thus kept on the sieve. Conversely, the leaves and the weaker parts of  
636 the stem might break into smaller pieces and hence, fall through the sieve holes.  
637 Figure 5S shows the efficiency of both methods for improving the compressive strength of  
638 concrete from 1.67 MPa in the presence of the lighter fractions in the mix and to 2.10 MPa if  
639 the lighter fractions were removed by air blown and to 2.73 MPa by sieving. This stresses the  
640 absolute need of removing light fractions if willing to prepare blocks with the highest  
641 possible compression strength.

642

643

### 644 **3.3 Life cycle Assessment (Granulo MG)**

645

#### 646 **3.3.1 Contribution analysis**

647 Only the contribution analysis of load-bearing block scenario is reported since it is very  
648 similar to the two other scenarios. The contribution analysis reported in Figure 6 is  
649 performed for a cultivation of miscanthus on a marginal and highly productive land that is  
650 not in competition with food production. It does not include the environmental benefit

651 linked to the valorisation of concrete blocks at the end of life, the environmental benefit of  
652 carbonation and the carbon storage in miscanthus.

653 As observed in LCA of hemp concrete [Arrigoni (2017), Prétot et al. 2014, Saez-Perez et al.  
654 2020, Sinka (2018) and Senga Kiessé et al. 2016], the contribution of the binder (mainly  
655 cement here) and the transport of the blocks represent the highest contribution to the  
656 climate change (more than 90% here). The predominance of the binder production and  
657 transport of the blocks is also noticed in the other impact categories (from 40% to 95% and  
658 65% on average). The miscanthus cultivation brings a noteworthy contribution especially on  
659 the marine eutrophication (30% to 40% according to the different scenarios) and particulates  
660 matter formation (30% to 40%) because of the nitrogen and phosphate emissions related to  
661 fertilisation and soil losses. The block end-of-life is noticeable regarding the ecotoxicity of  
662 freshwater (20% to 30%) and non-cancerogenic human toxicity (15% to 25%) because of the  
663 long-term emissions related to the infrastructure of the sorting plant. Finally, the last step  
664 having an important contribution is the infrastructure of block production which represents  
665 20% to 35% of the mineral, fossil, and renewable resources depletion.

666

667 Figure 6: Life cycle contribution analysis for a load-bearing scenario block cultivated on a  
668 high yield land not in competition with food production.

669

670 The influence of the block end-of-life is marginal in most of the impact categories excepted  
671 on the land-use (-10% to 20%), water depletion (-10% to 15%) and the mineral, fossil and  
672 resources depletion (-10% to 20%) as reported in Figure 7 for the load-bearing alternative.

673 The influence of carbonation and carbon storage on the climate change impact varies

674 between -45% to -70% according to the amount of miscanthus and cement in the different  
675 scenarios. The benefit is mainly due to the carbon sequestration in miscanthus (70% to 80%).

676

677 Figure 7: Influence of the carbonation, carbon sequestration and co-function on the life cycle  
678 impacts of a load-bearing scenario block cultivated on a high yield land not in competition  
679 with food production.

680

### 681 3.3.2 Comparisons

682

#### 683 3.3.2.1 Non-load bearing scenario blocks

684 Non-load-bearing blocks have a maximum of 4 MPa compression resistance at specific mass  
685 of about 1000 kg m<sup>-3</sup>. Figure 8 reports the results for all the environmental impacts  
686 calculated in this study. The results are normalised to the score of the brick. It means its  
687 impact is always set to 100%. If the result of the miscanthus alternative is below 100%, the  
688 miscanthus based scenario is better, and vice versa. The type of land used to cultivate  
689 miscanthus (high productivity or low productivity land) does not have a major influence on  
690 the comparison with the brick except for the marine eutrophication. This is due to the fact  
691 that the environmental impacts are mainly generated by the production of the block (50%  
692 on average with 28% because of the cement production) and the building of the wall (30%  
693 on average with 17% because of the transport of the block to the site and 5% each because  
694 of the mortar and the pallet used). Three impacts are in favour of the miscanthus  
695 alternatives while eight impacts are in favour of the conventional brick. Thus, unless a  
696 significant reduction of the cement use in the miscanthus block production or a reduction of  
697 the block weight thanks to a better design to improve structural properties, the miscanthus

698 reinforced block does not seem to be a better alternative compared to bricks for a non-load  
699 bearing wall.

700 It however has to be noticed that the miscanthus block allows a significant reduction of the  
701 climate change impact (around -30% for LPL to -40% HPL). Thus, regarding to the specific  
702 concern about this impact it has been decided to evaluate the environmental single score  
703 using the ReCiPe HA method in order to estimate if the better impact on the climate change  
704 can balance the worst results on other impact categories. The results displayed in Figure 9  
705 show that the environmental single scores of the miscanthus alternatives are equivalent to  
706 the conventional brick. An eco-design of the miscanthus reinforced block could thus allow to  
707 sufficiently improve the overall environmental impact.

708

709 Figure 8: Impact comparison of non-load bearing scenario miscanthus concrete block to  
710 brick.

711

712 Figure 9: Single score comparison of non-load bearing scenario miscanthus concrete block to  
713 brick.

714

715 Finally, it must be kept in mind that the previous results do not consider LUC. When  
716 considering that miscanthus was not cultivated on a land in competition with food for less  
717 than 20 years (dLUC scenario), the conclusion is similar. The climate change impact of  
718 miscanthus scenarios remain better (-25% for LPL to -35% for HPL) and the environmental  
719 single score is equivalent to that of the bricks. However, when considering that miscanthus is  
720 cultivated on a land in competition with food production, results are very different. The  
721 climate change impact is still better (-5% for LPL to -25% for HPL) but not enough to balance

722 the other impacts and, especially, the additional impact generated by the tropical land use. It  
723 leads to an environmental single score 2 to 3 times higher compared to the bricks. Despite  
724 the consideration of the iLUC in this study was not fine-tuned, the results show that this fact  
725 has to be kept in mind and refined before taking any short-term decision.

726 As previous studies made on hemp for non-load bearing wall [Heidari et al. 2019, Prétot et  
727 al. 2014], this study highlights the importance of not focusing the decision making on the  
728 climate change impact only. The benefit of the crop on the climate change impact can be  
729 compensated by other impact categories. Unlike previous studies made on hemp, this work  
730 questions the development of such an industry without thinking to indirect consequences  
731 driven by a global increase of the pressure on food production land.

732

### 733 3.3.2.2 Load-bearing scenario blocks

734 Load-bearing blocks have more than 6 MPa compression resistance at a specific mass of  
735 about 1000kg m<sup>-3</sup>.

736 Figure 10 shows that impacts are indeed driven by the production of the block (60% to 70%  
737 on average with 37% to 41% because of the cement) and the building of the wall (15% to  
738 20% on average with 11% to 18% because of the transport of the block to the site). The  
739 calculation of the single score and the evaluation of the LUC both confirm this conclusion. To  
740 be competitive from an environmental point of view, the load-bearing scenario miscanthus  
741 based block should: (1) reduce the amount of cement in the formulation (2) and/or modify  
742 the type of cement required for a more environmentally friendly one (3) and/or improve the  
743 design of the block in order to increase the ratio mass/surface of wall.

744

745 Figure 10: Impact score comparison of a load bearing scenario miscanthus concrete block to  
746 a 100% concrete block.

747

#### 748 **4- Conclusions**

749 To produce lightweight load-bearing concrete blocks using miscanthus stem fragments as  
750 aggregates in a single mixing method turned out to be impossible, even trying to optimize  
751 the concrete formulation, the effect of miscanthus genotypes, the fragment size and to  
752 remove light elements like leaf pieces. The results show that genotypes and size of  
753 miscanthus fragments play an important role on the mechanical properties of the final  
754 products, mainly due to the presence or not of light elements such as leaves and sheath.

755 When comparing genotypes with the same leaf/stem ratio, it was not possible to see a  
756 correlation between the biochemical composition of the stem and the compressive strength  
757 of the blocks. A probable explanation is the small variation of biochemical composition  
758 between genotypes.

759 Miscanthus-based blocks were compared to conventional alternatives using life cycle  
760 analysis tools and the source of impacts were identified in a perspective of eco-design.

761 Although the study must be refined regarding the integration of the heat and acoustic  
762 insulation, the first results of the comparison showed that, without improvement, the use of  
763 miscanthus block is not competitive compared to conventional load-bearing alternatives  
764 (concrete block and lightweight pumice block). However, compared to a non-load bearing  
765 alternative (light clay brick), block integrating miscanthus can be competitive from a global  
766 environmental point of view thanks to good performances on the climate change impact (-  
767 30% to 40%). As previous studies made on hemp showed, this study highlighted the  
768 importance of not focusing the decision making on only the climate change impact for

769 developing biobased concretes. The present work also pointed out the risk of decreasing the  
770 environmental performances when cultivating the crop on land in competition with food,  
771 because of the consequences of indirect consequences of Land Use Change (iLUC), a topic  
772 that was not discussed in a previous study about hemp. Finally, the productivity of land (low  
773 or high) where miscanthus was cultivated had no major influence on the results excepted  
774 when iLUC are considered. Most of the impacts were driven by the use of cement and the  
775 transportation of the blocks. However, this LCA study had three main limitations: heat and  
776 acoustic insulation performances were not considered, the methodology to estimate was  
777 not developed for permanent crop such as miscanthus and 1 ha of miscanthus cultivated in  
778 competition with food production replaces 1 ha of primary forest.  
779 An ecodesign of the blocks should thus be oriented on the reduction of cement use as well  
780 as on reducing the mass of a block while keeping the same function.

781

## 782 **5- Acknowledgements**

783 This work was supported by the program Investments for the Future (grant ANR-11-BTBR-  
784 0006-BFF) managed by the French National Research Agency. Authors are grateful to the  
785 following agriculture specialist for their help in building the scenarios: Alain Besnard and  
786 Sylvain Marsac from Arvalis, Pierre Malvoisin from Aelred, Thierry Jacquet, Magali Berthou  
787 and Claire Brami from Phytoresource and Chantal Loyce from AgroParisTech.

788

## 789 **6- Author contributions**

790 Colin Jury: Conceptualization; Investigation; Jordi Girones: Investigation, Writing - original  
791 draft; Loan T. T. Vo: Investigation, Writing - original draft; Erika Di Giuseppe: Investigation;  
792 Grégory Mouille: Investigation; Emilie Gineau: Investigation; Stéphanie Arnoult: Investigation,

793 Maryse Brancourt-Hulmel: Investigation; Catherine Lapierre: investigation; Laurent Cézard:  
794 investigation; Patrick Navard: Conceptualization, Writing-original draft.

795

## 796 **7- References**

797

798 Acikel H. 2011. The use of miscanthus (*Giganteus*) as a plant fiber in concrete production,  
799 *Sci. Res. Essays* 6, 2660-2667. <https://doi.org/10.5897/SRE10.1139>

800 Alengaram U.J., Al Muhit B.A. bin Jumaat M.Z. 2013. Utilization of oil palm kernel shell as  
801 lightweight aggregate in concrete – A review, *Constr. Build. Mater.* 38, 161–172.

802 <https://doi.org/10.1016/j.conbuildmat.2012.08.026>

803 Amziane S., Sonebi M. 2016. Overview on biobased building material made with plant  
804 aggregate, *RILEM Tech. Lett.* 1, 31-38. <https://doi.org/10.21809/rilemtechlett.2016.9>

805 Arrigoni A., Pelosato R., Melia P., Ruggieri G., Sabbadini S., GiovanniDotelli G. 2017. Life cycle  
806 assessment of natural building materials: the role of carbonation, mixture components and  
807 transport in the environmental impacts of hempcrete blocks, *Journal of Cleaner Production*,  
808 149, 1051-1061 <https://doi.org/10.1016/j.jclepro.2017.02.161>

809 Audsley E., Brander M., Chatterton J., Murphy-Bokern D., Webster C., Williams A. 2009. How  
810 Low Can We Go? An Assessment of Greenhouse Gas Emissions from the UK Food System and  
811 the Scope to Reduce Them by 2050, World-Wide WFund-UK.

812 <http://dspace.lib.cranfield.ac.uk/handle/1826/6503> (accessed 08 May 2021)

813 Barbieri V., Lassinantti Gualtieri M., Siligardi C. 2020. Wheat husk: A renewable resource for  
814 bio-based building materials, *Constr. Build. Mater.* 251, 118909.

815 <https://doi.org/10.1016/j.conbuildmat.2020.118909>



816 Bederina M., Gotteicha M., Belhadj B., Dheily R.M., Khenfer M.M., Queneudec M. 2012.  
817 Drying shrinkage studies of wood sand concrete – Effect of different wood treatments,  
818 *Constr. Build. Mater.* 36, 1066–1075. <https://doi.org/10.1016/j.conbuildmat.2012.06.010>

819 Boix E., Georgi F., Navard P. 2016. Influence of alkali and Si-based treatments on the physical  
820 and chemical characteristics of miscanthus stem fragments, *Industrial Crops and Products*,  
821 91, 6–14. <https://doi.org/10.1016/j.indcrop.2016.06.030>

822 Boix E., Ginau E., Narciso J.O., Höfte H., Mouille G., Navard P. 2020. Influence of chemical  
823 treatments of miscanthus stem fragments on polysaccharide release in the presence of  
824 cement and on the mechanical properties of bio-based concrete materials, *Cement and*  
825 *Concrete Composites*, 105, 103429. <https://doi.org/10.1016/j.cemconcomp.2019.103429>

826 Boulekbache B., Hamrat M., Chemrouk M., Amziane S. 2010. Flowability of fibre-reinforced  
827 concrete and its effect on the mechanical properties of the material, *Construction and*  
828 *Building Materials* 24, 1664-1671. <https://doi.org/10.1016/j.conbuildmat.2010.02.025>

829 Chabannes M., Garcia-Diaz E., Clerc L., Bénézet J.-C., Becquart F. 2018. Lime Hemp and Rice  
830 Husk-Based Concretes for Building Envelopes, Springer International Publishing.  
831 <https://doi.org/10.1007/978-3-319-67660-9>

832 Chen Y., Yu Q.L., Brouwers H.J.H. 2017. Acoustic performance and microstructural analysis of  
833 bio-based lightweight concrete containing miscanthus, *Construct. Build. Mater.* 157, 839–  
834 851. <https://doi.org/10.1016/j.conbuildmat.2017.09.161>

835 Chen Y.X., Wu F., Yu Q., Brouwers H.J.H. 2020. Bio-based ultra-lightweight concrete applying  
836 miscanthus fibers: Acoustic absorption and thermal insulation, *Cement and Concrete*  
837 *Composites* 114, 103829. <https://doi.org/10.1016/j.cemconcomp.2020.103829>

838 Chupin L., Soccalingame L., De Ridder D., Gineau E., Mouille G., Arnoult S., Brancourt-Hulmel  
839 M., Lapierre C., Vincent L., Mija A., Corn S., Le Moigne N., Navard P. 2020. Thermal and  
840 dynamic mechanical characterization of miscanthus stem fragments: effects of genotypes,  
841 positions along the stem and their relation with biochemical and structural characteristics,  
842 *Industrial Crops & Products* 156, 112863. <http://dx.doi.org/10.1016/j.indcrop.2020.112863>

843 Çomak B., Bideci A., Salli Bideci Ö. 2018. Effects of hemp fibers on characteristics of cement  
844 based mortar, *Constr. Build. Mater.* 169, 794–799.  
845 <https://doi.org/10.1016/j.conbuildmat.2018.03.029>

846 Courard L., Parmentier V. 2017. Carbonated miscanthus mineralized aggregates for reducing  
847 environmental impact of lightweight concrete blocks, *Sust. Build.* 2, 3.  
848 <https://doi.org/10.1051/sbuild/2017004>

849 Dixit A., Pang S.D., Kang S.-H., Moon J. 2019. Light weight structural cement composites with  
850 expanded polystyrene (EPS) for enhanced thermal insulation, *Cement and Concrete*  
851 *Composites* 102, 185–197. <https://doi.org/10.1016/j.cemconcomp.2019.04.023>

852 European Commission 2010. Joint Research Centre - Institute for Environment and  
853 Sustainability: International Reference Life Cycle Data System (ILCD) Handbook - General  
854 guide for Life Cycle Assessment - Detailed guidance. First edition March 2010. EUR 24708 EN.  
855 Luxembourg. Publications Office of the European Union; 2010

856 European Commission 2012. Joint Research Centre, Institute for Environment and  
857 Sustainability.Characterisation factors of the ILCDRecommended Life Cycle Impact  
858 Assessment methods.Database and Supporting Information.First edition. February 2012.  
859 EUR 25167. Luxembourg. Publications Office of the European Union; 2012

860 Ferchaud F. Unpublished. UMR Transfrontalière BioEcoAgro - INRAE AgrolImpact. Pôle du  
861 Griffon. 180 rue Pierre-Gilles de Gennes, France. Compilation of data from Clifton-Brown J.C.  
862 et al. 2007. Carbon mitigation by the energy crop, Miscanthus. *Glob. Change Biol.* 13, 2296-  
863 2307; Schneckenberger K., Kuzyakov, Y. 2007. Carbon sequestration under Miscanthus in  
864 sandy and loamy soils estimated by natural <sup>13</sup>C abundance. *J. Plant Nutr. Soil Sci.* 170, 538-  
865 542; Zatta A. et al. 2014. Land use change from C3 grassland to C4 Miscanthus: effects on  
866 soil carbon content and estimated mitigation benefit after six years. *Global Change Biology*  
867 *Bioenergy* 6, 360-370; Hansen E.M. et al. 2004. Carbon sequestration in soil beneath long-  
868 term Miscanthus plantations as determined by <sup>13</sup>C abundance. *Biomass and Bioenergy* 26,  
869 97-105; Poeplau C., Don A. 2014. Soil carbon changes under Miscanthus driven by C-4  
870 accumulation and C-3 decomposition - toward a default sequestration function. *Global*  
871 *Change Biology Bioenergy* 6, 327-338; Ferchaud F., Mary B., Rupngam T., Chenu C. 2020.  
872 Changes in soil carbon stocks and distribution under perennial and annual bioenergy crops,  
873 EGU General Assembly 2020, Online, 4–8 May 2020, EGU2020-20118,  
874 <https://doi.org/10.5194/egusphere-egu2020-20118>, 2020

875 Fiche de Déclaration Environnementale et Sanitaire de la brique de cloison. 2020. Terre et  
876 Pierre <https://www.base-inies.fr/iniesV4/dist/consultation.html?id=14172> (accessed 22  
877 November 2021)

878 Fiche de Déclaration Environnementale et Sanitaire. Maçonnerie de Blocs CLIMAT® collés à  
879 joints minces (Bloc de béton de pierre ponce). Avril 2012. Alkern [www.alkern.fr](http://www.alkern.fr) (accessed 10  
880 December 2020)

881 Flysjö A, Cederberg C, Henriksson M, Ledgard S. 2012. The interaction between milk and  
882 beef production and emissions from land use change and critical considerations in life cycle

883 assessment and carbon footprint studies of milk. *Journal of Cleaner Production* 28, 134-142.  
884 <https://doi.org/10.1016/j.jclepro.2011.11.046>

885 Fusi A., Bacenetti J., Proto A.R., Tedesco D.E.A., Pessina, D., Facchinetti, D. 2021. Pellet  
886 production from miscanthus: energy and environmental assessment. *Energies*. 14, 73-73.  
887 <https://doi.org/10.3390/en14010073>

888 Girones J., Vo L., Arnoult S., Brancourt-Hulmel M., Navard P. 2016. Miscanthus stem  
889 fragment - Reinforced polypropylene composites: Development of an optimized preparation  
890 procedure at small scale and its validation for differentiating genotypes, *Polym. Test.* 55,  
891 166–172. <https://doi.org/10.1016/j.polymertesting.2016.08.023>

892 Goedkoop M., Heijungs R., Huijbregts M., De Schryver A., Struijs J., Van Zelm R. 2012. ReCiPe  
893 2008 : A life cycle impact assessment method which comprises harmonized category  
894 indicators at the midpoint and the endpoint level, First edition (revised).  
895 <https://www.rivm.nl/en/life-cycle-assessment-lca/recipe>. Accessed 22 November 2021.

896 Heidari M.D., Lawrence M., Blanchet P., Amor B. 2019. Regionalised Life Cycle Assessment of  
897 Bio-Based Materials in Construction; the Case of Hemp Shiv Treated with Sol-Gel Coatings,  
898 *Materials* 12, 2987 <https://doi.org/10.3390/ma12182987>

899 Ho-Yue-Kuang S., Alvarado C., Antelme S., Bouchet B., Cezard, L., Le Bris P., Legee F., Maia-  
900 Grondard A., Yoshinaga A., Saulnier L., Guillon F., Sibout R., Lapierre C., Chateigner-Boutin  
901 A.L. 2016. Mutation in *Brachypodium* caffeic acid O-methyltransferase 6 alters stem and  
902 grain lignins and improves straw saccharification without deteriorating grain quality, *J Exp*  
903 *Bot.* 67, 227–237. <https://doi.org/10.1093/jxb/erv446>

904 Jami, T., Karade S.R., Singh L.P. 2019. A review of the properties of hemp concrete for green  
905 building applications, *Journal of Cleaner Production* 239, 117852  
906 <https://doi.org/10.1016/j.jclepro.2019.117852>

907 Kaak K., Schwarz K.U. 2001. Morphological and mechanical properties of *Miscanthus* in  
908 relation to harvesting, lodging, and growth conditions. *Industrial Crops and Products* 14,  
909 145–154. [https://doi.org/10.1016/S0926-6690\(01\)00078-4](https://doi.org/10.1016/S0926-6690(01)00078-4)

910 Kaak K., Schwarz K.-U., Brander P.E. 2003. Variation in morphology, anatomy and chemistry  
911 of steams of *Miscanthus* genotypes in mechanical properties. *Industrial Crops and Products*  
912 17, 131–142. [https://doi.org/10.1016/S0926-6690\(02\)00093-6](https://doi.org/10.1016/S0926-6690(02)00093-6)

913 Karade S.R., Irle M., K. Maher K., 2006. Influence of granule properties and concentration on  
914 cork-cement compatibility, *Holz Als Roh- Und Werkst.* 64, 281–286.  
915 <https://doi.org/10.1007/s00107-006-0103-2>

916 Krzyżaniak M., Stolarski M.J., Warmiński K. 2020. Life cycle assessment of giant miscanthus:  
917 production on marginal soil with various fertilisation treatments, *Energies* 13, 1931.  
918 <https://doi.org/10.3390/en13081931>

919 Lameiras R., Barros J.A.O., Azenha M. 2015. Influence of casting condition on the anisotropy  
920 of the fracture properties of Steel Fibre Reinforced Self-Compacting Concrete (SFRSCC),  
921 *Cement & Concrete Composites* 59, 60–76.  
922 <http://dx.doi.org/10.1016/j.cemconcomp.2015.03.008>

923 Lask J., Wagner M., Trindade L.M., Lewandowski I. 2019. Life cycle assessment of ethanol  
924 production from miscanthus: A comparison of production pathways at two European sites.  
925 *GCB Bioenergy* 11, 269-288. <https://doi.org/10.1111/gcbb.12551>

926 Li P., Wu H., Liu Y., Yang J., Fang Z., Lin B. 2019. Preparation and optimization of ultra-light  
927 and thermal insulative aerogel foam concrete, *Construction and Building Materials* 205, 529–  
928 542. <https://doi.org/10.1016/j.conbuildmat.2019.01.212>

929 Liu L.F., Li H.Q., Lazzaretto A., Manente G., Tong C.Y., Bin Liu Q., Li N.P. 2017. The  
930 development history and prospects of biomass-based insulation materials for buildings,  
931 *Renew. Sustain. Energy Rev.* 69, 912–932. <https://doi.org/10.1016/j.rser.2016.11.140>

932 L. Vo L.T.T., Navard P. 2016. Treatments of plant biomass for cementitious building materials  
933 – A review, *Construction and Building Materials*, 121, 161–176.  
934 <http://dx.doi.org/10.1016/j.conbuildmat.2016.05.125>

935 Méchin V., Laluc A., Legée F., Cézard L., Denoue D., Barrière Y., Lapierre C. 2014. Impact of  
936 the brown-midrib bm5 mutation on maize lignins. *Journal of Agricultural and Food Chemistry*  
937 62, 5102–5107. <https://doi.org/10.1021/jf5019998>

938 Merta I., Tschegg E.K., 2013. Fracture energy of natural fibre reinforced concrete, *Constr.*  
939 *Build. Mater.* 40, 991–997. <https://doi.org/10.1016/j.conbuildmat.2012.11.060>

940 Ntimugura, F., Vinai, R., Harper, A., Walker P. 2020. Mechanical, thermal, hygroscopic and  
941 acoustic properties of bio-aggregates – lime and alkali - activated insulating composite  
942 materials: A review of current status and prospects for miscanthus as an innovative resource  
943 in the South West of England, *Sustainable Materials and Technologies* 26, e00211.  
944 <https://doi.org/10.1016/j.susmat.2020.e00211>

945 Onuaguluchi, O., Banthia N. 2016. Plant-based natural fibre reinforced cement composites: A  
946 review, *Cement and Concrete Composites* 68, 96-108  
947 <https://doi.org/10.1016/j.cemconcomp.2016.02.014>

948 Ozyurt N., Mason T.O., Shah S.P. 2007. Correlation of fiber dispersion, rheology and  
949 mechanical performance of FRCs, *Cement and Concrete Composites* 29, 70-79.  
950 <https://doi.org/10.1016/j.cemconcomp.2006.08.006>

951 Pereira Dias P., Waldmann D. 2020. Optimisation of the mechanical properties of *Miscanthus*  
952 lightweight concrete, *Construction and Building Materials* 258, 119643  
953 <https://doi.org/10.1016/j.conbuildmat.2020.119643>

954 Peric M., Komatina M., Dragi Antonijevic D., Branko Bugarski B., Dželetovic Ž. 2018. Life cycle  
955 impact assessment of miscanthus crop for sustainable household heating in Serbia, *Forests*  
956 9, 654. <https://doi.org/10.3390/f9100654>

957 Pommer, K., Pade C., 2005. Guidelines - Uptake of carbon dioxide in the life cycle inventory  
958 of concrete, October 2005. Nordic Innovation Centre Project. NI-project 03018 CO2 Uptake  
959 During the Concrete Life Cycle. Danish Technological Institute. ISBN: 87-7756-757-9.  
960 <https://www.dti.dk> (accessed 09 May 2021)

961 Prétot S., Collet F., Garnier C. 2014. Life cycle assessment of a hemp concrete wall: impact of  
962 thickness and coating, *Building and Environment*, 72C, 223-231.  
963 <https://doi.org/10.1016/j.buildenv.2013.11.010>. hal-00916557

964 Prusty, J.K., Patro, S.K., Basarkar S.S. 2016. Concrete using agro-waste as fine aggregate for  
965 sustainable built environment – A review, *Int. J. Sustain. Built Environ.* 5, 312–333.  
966 <https://doi.org/10.1016/j.ijbsbe.2016.06.003>

967 Pude R. 2003. Neue sichere Anbaumethoden von *Miscanthus* in Europa. In: *Berichte über*  
968 *Landwirtschaft*, Bd. 81 (3), Landwirtschaftsverlag Münster-Hiltrup, 405–415

969 Pude, R., Treseler C.H. 2002. Neue Ansprüche an Miscanthus – Genotypen bei stofflicher  
970 Nutzung. In: Pude, R. (ed.), Anbau und Verwertung von Miscanthus in Europa. Beiträge zu  
971 Agrarwissenschaften Bd. 26.; Verlag Wehle, Bad Neuenahr, 13–17

972 Pude, R., Treseler C.H., Noga G. 2004. Morphological, Chemical and Technical Parameters of  
973 Miscanthus Genotypes, *Journal of Applied Botany* 78, 58–63

974 Pude R., Treseler C.H., Trettin R., Noga G. 2005. Suitability of Miscanthus Genotypes for  
975 Lightweight Concrete. *Die Bodenkultur* 63, 56 (1)

976 Saez-Perez M.P., Brümmer M., Duran-Suarez J.A. 2020. A review of the factors affecting the  
977 properties and performance of hemp aggregate concretes, *Journal of Building Engineering*  
978 31, 101323. <https://doi.org/10.1016/j.jobe.2020.101323>

979 Schmidt J., Reinhard J, Weidema B. (2011). Modelling of Indirect Land Use Change in LCA.  
980 Report v2.2.-0. LCA Consultants, Aalborg (Denmark). [https://lca-](https://lca-net.com/projects/show/indirect-land-use-change-model-iluc/)  
981 [net.com/projects/show/indirect-land-use-change-model-iluc/](https://lca-net.com/projects/show/indirect-land-use-change-model-iluc/) (accessed 09 May 2021)

982 Senga Kiese T., Ventura A., Van Der Werf H. M.G.; Cazacliu B., Idir R., Andrianandraina A.  
983 2016. Introducing economic actors and their possibilities for action in LCA using sensitivity  
984 analysis: Application to hemp-based insulation products for building applications, *Journal of*  
985 *Cleaner Production* 142, 3905-3916. [https://doi.org 10.1016/j.jclepro.2016.10.069](https://doi.org/10.1016/j.jclepro.2016.10.069)

986 Sibout R., Le Bris P., Legée F., Cézard L., Renault H., Lapiere C. 2016. Structural redesigning  
987 arabidopsis lignins into alkali-soluble lignins through the expression of p-coumaroyl-  
988 coA:monolignol transferase PMT. *Plant Physiol*, 170, 1358-1366. [https://doi.org](https://doi.org/10.1104/pp.15.01877)  
989 [10.1104/pp.15.01877](https://doi.org/10.1104/pp.15.01877)



990 Sinka M., Van den Heede P., De Belie N., Bajare D., Sahmenko G., Korjakinsa A. 2018.  
991 Comparative life cycle assessment of magnesium binders as an alternative for hemp  
992 concrete, *Resources, Conservation and Recycling* 133, 288-299.  
993 <https://www.sciencedirect.com/science/article/abs/pii/S0921344918300831?via%3Dihub>

994 Tadele D., Roy P., Defersha F., Misra M., Mohanty A.K. 2019. Life cycle assessment of  
995 renewable filler material (biochar) produced from perennial grass (*Miscanthus*), *AIMS Energy*  
996 7(4), 430–440. <https://doi.org/10.3934/energy.2019.4.430>

997 Tonoli G.H.D., Belgacem M.N., Siqueira G., Bras J., Savastano H., Rocco Lahr F.A. 2013.  
998 Processing and dimensional changes of cement based composites reinforced with surface-  
999 treated cellulose fibres, *Cem. Concr. Compos.* 37, 68–75.  
1000 <http://dx.doi.org/10.1016/j.cemconcomp.2012.12.004>

1001 Turgut P. 2007. Cement composites with limestone dust and different grades of wood  
1002 sawdust, *Build. Environ.* 42, 3801–3807. <https://doi.org/10.1016/j.buildenv.2006.11.008>

1003 Waldmann D., Thapa V., Dahm F., Faltz C. 2016. Masonry Blocks from Lightweight Concrete  
1004 on the Basis of *Miscanthus* as Aggregates. Chapter 23. In S. Barth et al. (eds.), *Perennial*  
1005 *Biomass Crops for a Resource-Constrained*. Springer. [https://doi.org/10.1007/978-3-319-](https://doi.org/10.1007/978-3-319-44530-4_23)  
1006 [44530-4\\_23](https://doi.org/10.1007/978-3-319-44530-4_23)

1007 Yang Z., Huo, Z., Chen, W., Li Y., He R., 2019. Study on Fabrication and Characteristic of  
1008 Green Concrete by Using Natural Graded Gravel. *IOP Conf. Ser.: Earth Environ. Sci.* 233,  
1009 022014. <https://doi.org/10.1088/1755-1315/233/2/022014>

1010 Yesufu J., McCalmont J., Clifton-Brown J.C., Williams P., Hyland J., Gibbons J., Styles D. 2020.  
1011 Consequential life cycle assessment of miscanthus livestock bedding, diverting straw to  
1012 bioelectricity generation. *GCB Bioenergy* 12, 39-53. <https://doi.org/10.1111/gcbb.12646>

1013 Zapater, M., Catterou, M., Mary, B., Ollier, M., Fingar, L., Mignot, E., Ferchaud, F., Strullu, L.,  
1014 Dubois, F., Brancourt-Hulmel, M. A2017. Single and Robust Critical Nitrogen Dilution Curve  
1015 for *Miscanthus x giganteus* and *Miscanthus sinensis*. *BioEnergy Research*. 10, 115-129.  
1016 <https://doi.org/10.1007/s12155-016-9781-8>

1017 Zeng Q., Mao T., Li H., Peng Y. 2018. Thermally insulating lightweight cement-based  
1018 composites incorporating glass beads and nano-silica aerogels for sustainably energy-saving  
1019 buildings, *Energy & Buildings* 174, 97–110. <https://doi.org/10.1016/j.enbuild.2018.06.031>

1020 Zub, H.W., Arnoult, S., Brancourt-Hulmel, M., 2011. Key traits for biomass production  
1021 identified in different *Miscanthus* species at two harvest dates, *Biomass Bioenergy* 35, 637–  
1022 651. <https://doi.org/10.1016/j.biombioe.2010.10.020>

1023

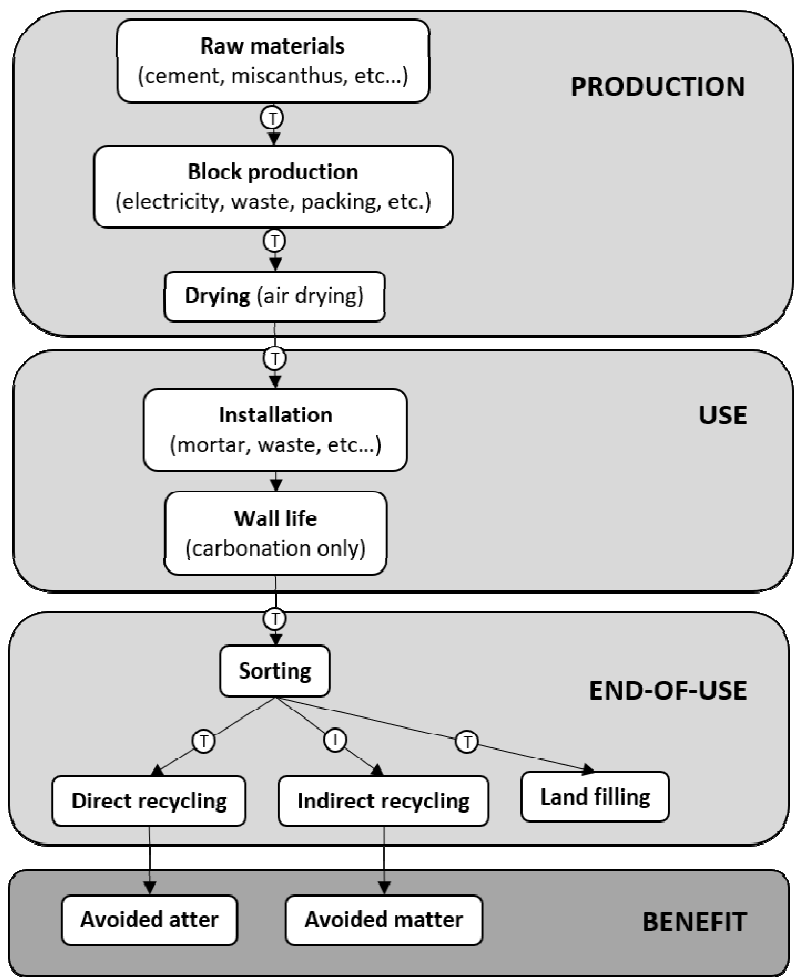


Figure 1: LCA system boundaries.

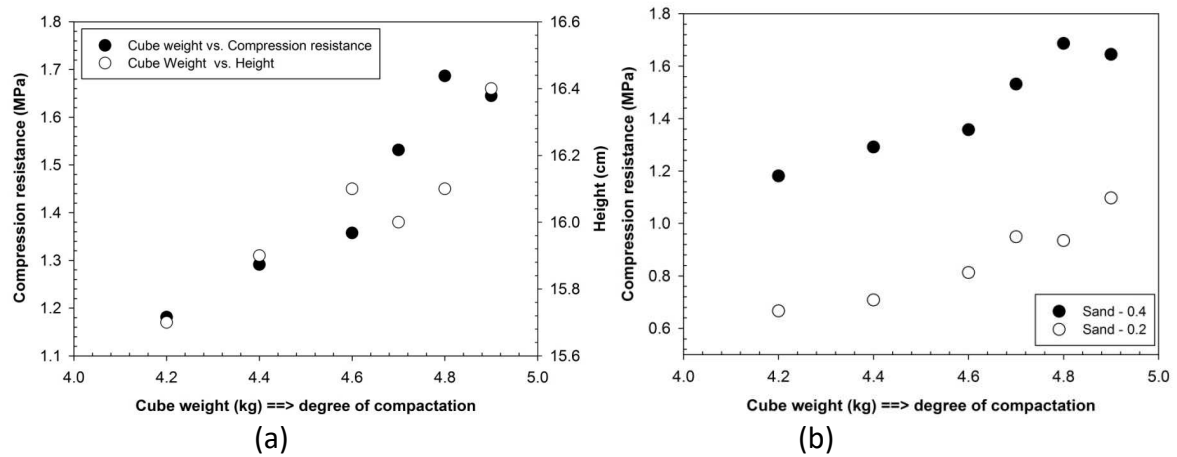


Figure 2: (a) Relationship between compressive strength/height of concrete block (sand 0-4) after 7 days and its weight (the initial height was 15 cm) and (b) mechanical properties of concrete blocks prepared with sand granulometry of 0-2 and 0-4.

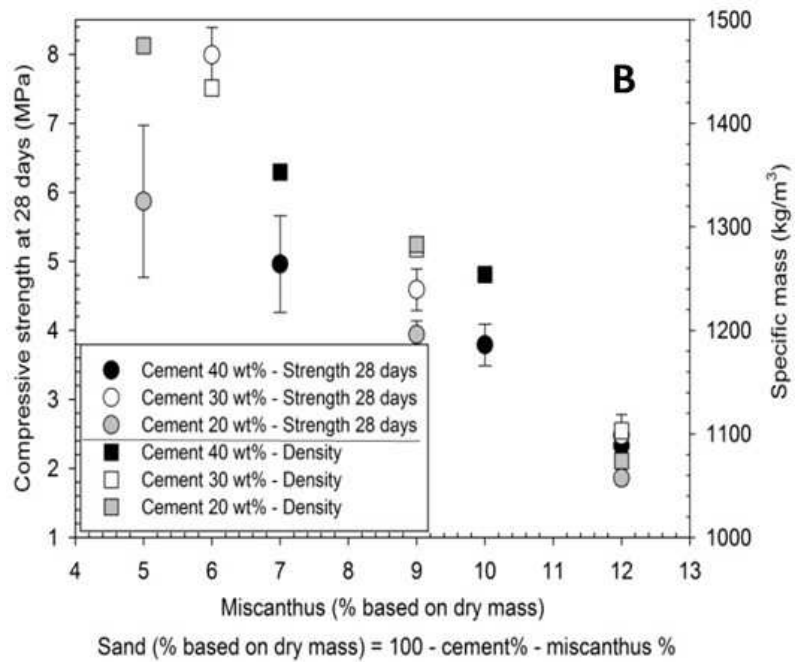
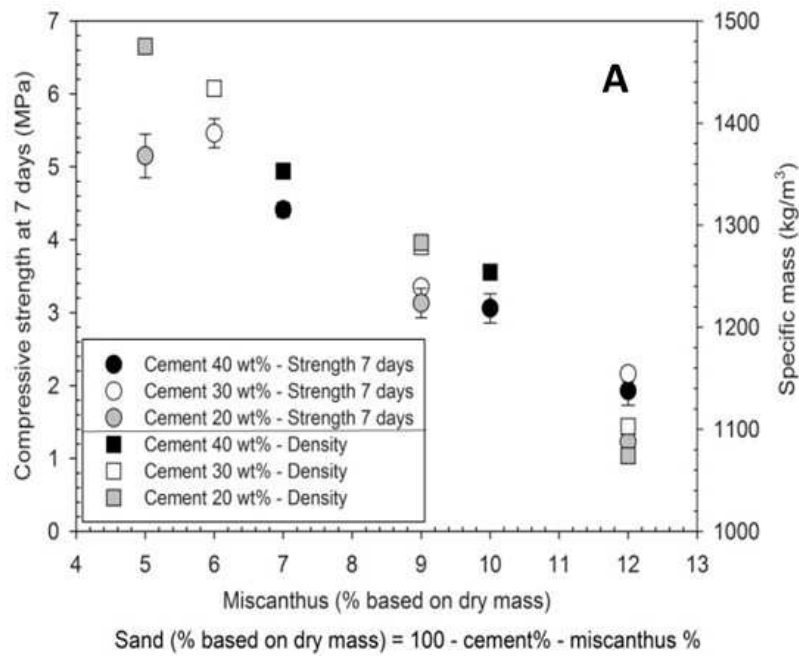


Figure 3: Compressive strengths vs. specific mass of the concrete blocks after (a) 7 days and (b) 28 days.

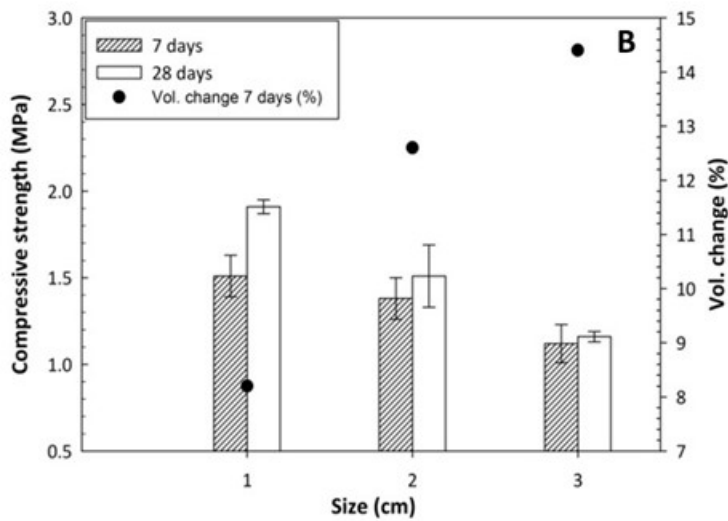
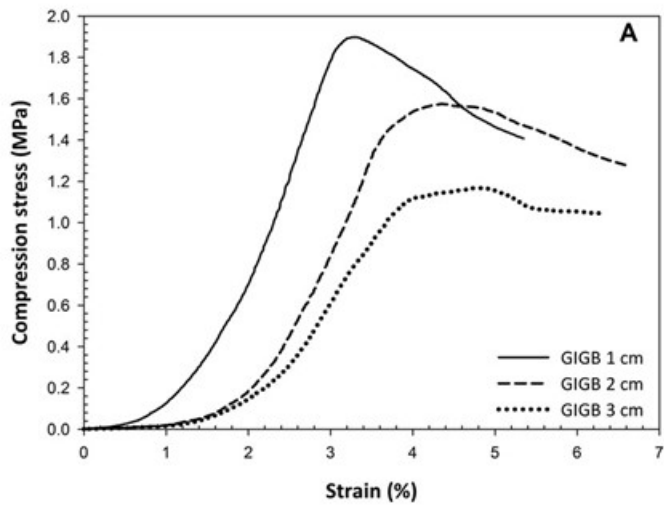
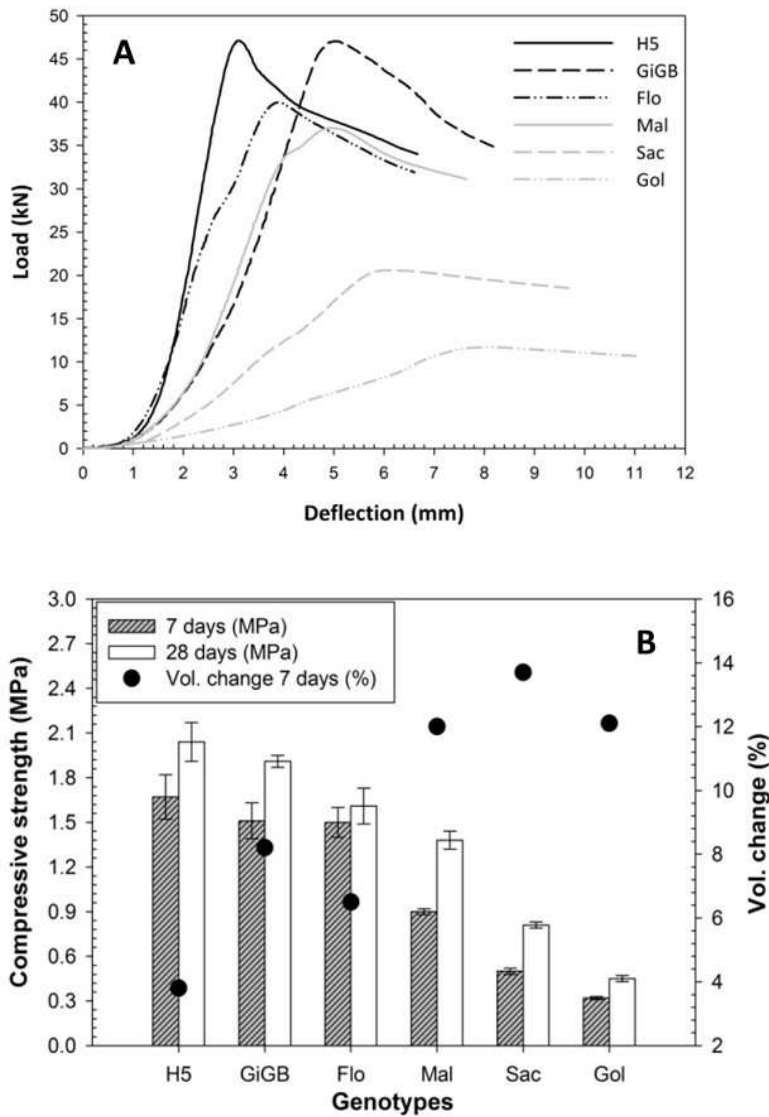


Figure 4: (a) Stress-strain curves at 28 days of the concretes reinforced with fibers from different sizes and (b) their compressive strengths at 7 and 28 days (bars) and volume change at 7 days (●).



**Figure 5:** (a) Compressive load – deformation curves at 28 days of the concretes reinforced with fragments from different genotypes and (b) their compressive strengths at 7 and 28 days (bars) and volume change at 7 days (●).

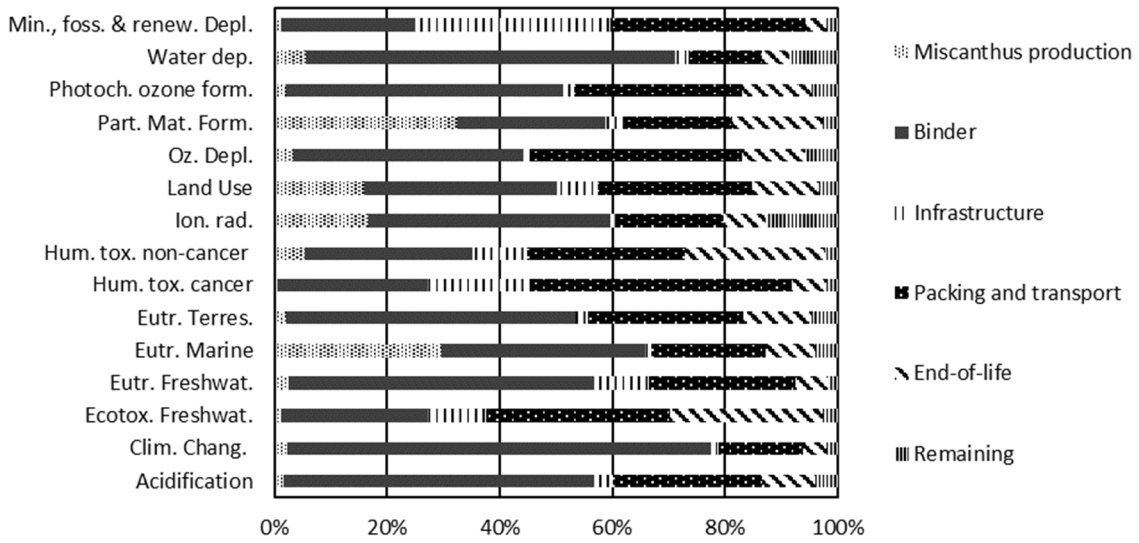
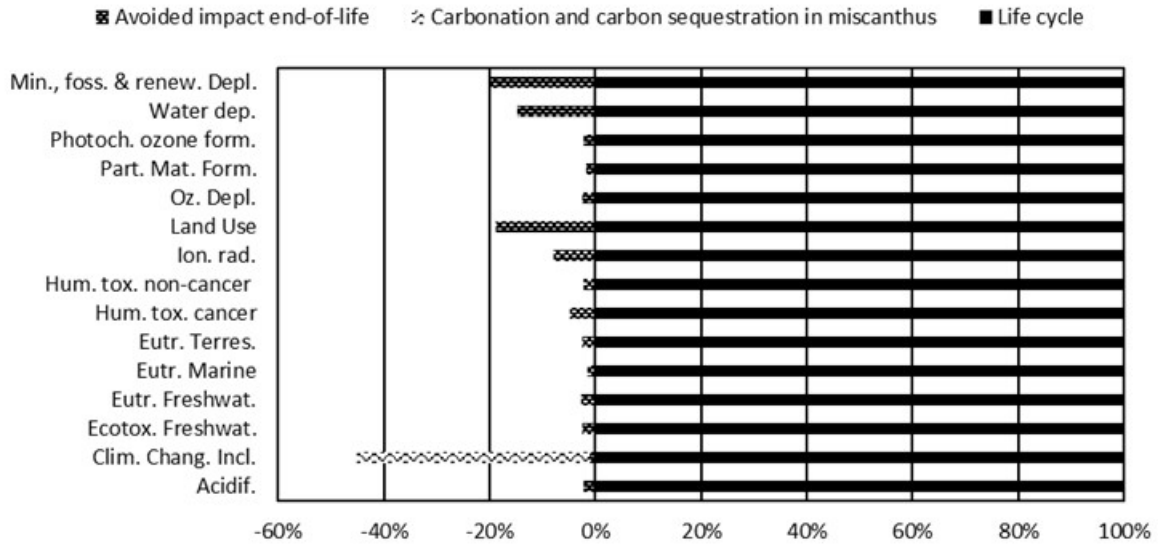


Figure 6: Life cycle contribution analysis for a load-bearing scenario block cultivated on a high yield land not in competition with food production.





**Figure 7:** Influence of the carbonation, carbon sequestration and co-function on the life cycle impacts of a load-bearing scenario block cultivated on a high yield land not in competition with food production.

a

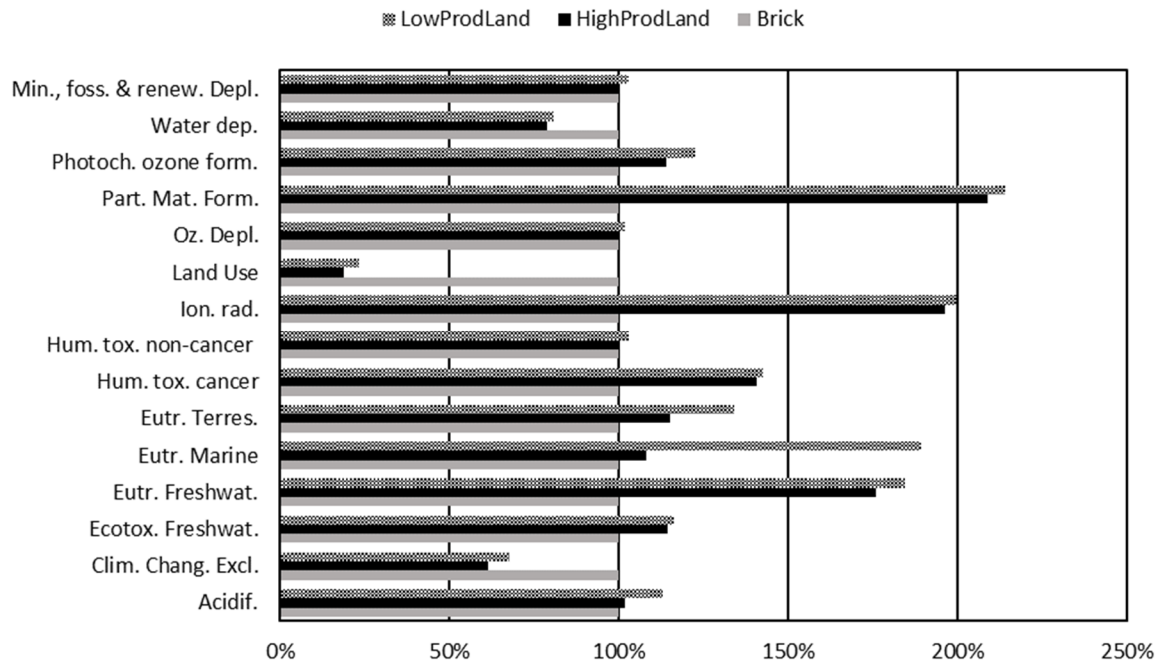


Figure 8: Impact comparison of non-load bearing scenario miscanthus concrete block to brick.

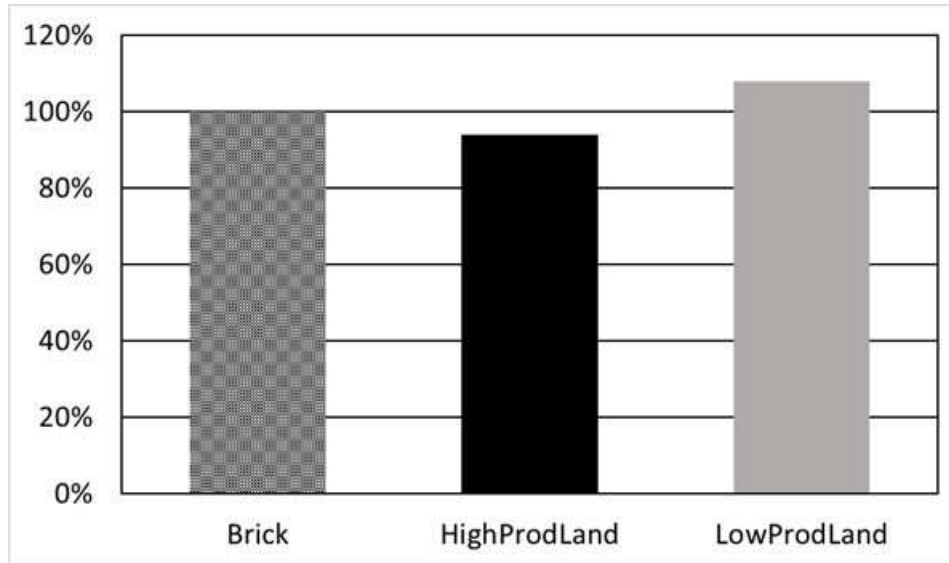
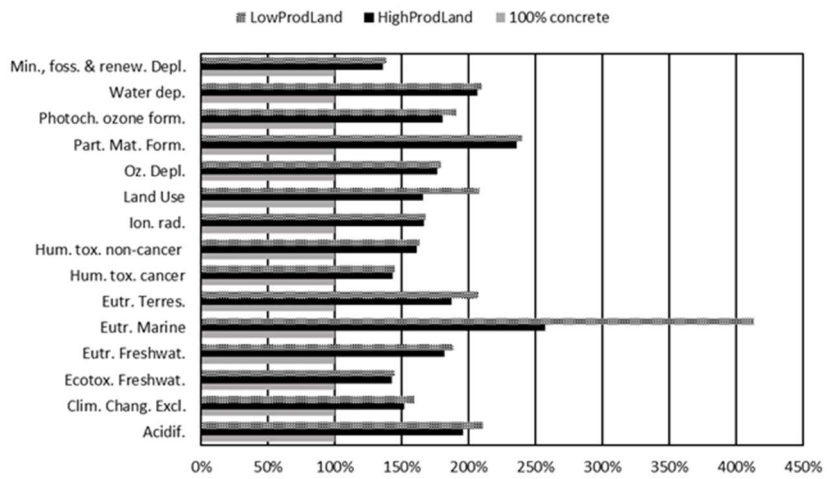


Figure 9: Single score comparison of non-load bearing scenario miscanthus concrete block to brick.



**Figure 10:** Impact score comparison of a load bearing scenario miscanthus concrete block to a 100% concrete block.

LCA Single score

